Working Report 2007-47

Petrology, Petrophysics and Fracture Mineralogy of the Drill Core Sample OL-KR22 and OL-KR22B

Seppo Gehör
Aulis Kärki
Markku Paananen

June 2007

POSIVA OY
FI-27160 OLKILUOTO, FINLAND
Tel +358-2-8372 31
Fax +358-2-8372 3709

Working Report 2007-47

Petrology, Petrophysics and Fracture Mineralogy of the Drill Core Sample OL-KR22 and OL-KR22B

Seppo Gehör

Aulis Kärki

Kivitieto Oy

Markku Paananen

Geological Survey of Finland

June 2007

ABSTRACT

This report represents the results of the studies dealing with the drill core samples OL-KR22 and OL-KR22B, drilled in the south eastern part of the Olkiluoto study site. Lithological properties, whole rock chemical compositions, mineral compositions, textures, petrophysical properties and low temperature fracture infill minerals are described.

The drill holes start in the diatexitic gneiss domain and intersect down to length of 360 m rather monotonous diatexitic gneisses which are intruded by a couple of wide pegmatitic granite dykes and have several homogeneous mica gneiss and mafic gneiss subsections. Below that, down to the length of 422 m, a fluctuating section of veined gneisses with narrow mica gneiss interbeds is located. The lowermost part of the core sample is composed of rather homogeneous mica gneisses with various migmatite subsections

Detailed Petrological properties have been analysed from 12 samples. The T series is represented by six diatexitic gneiss samples and one veined gneiss sample which give an extensive overview of the whole series. Only the extremely basic and acidic types are excluded. SiO_2 concentration varies from 58%, analysed from biotite rich veined gneiss, to ca. 73%, analysed from light, diatexitic gneiss. One mafic gneiss sample is included into the S-series. The sample is the most mafic example analysed from this group and contains only 43% SiO_2 and ca. 10% CaO. The P series is represented by one TGG gneiss, one diatexitic gneiss and two mica gneiss samples. As typical for the P series, the content of phosphorus exceeds 0.4%, given as P_2O_5, in every of those while SiO_2 concentration varies between 50% and 65%.

Petrophysical properties were studied from 12 samples. The parameters measured were density, magnetic susceptibility, natural remanet magnetization, electrical resistivity, P-wave velocity and porosity.

Borehole represents a relatively intensively fractured rock down to the core length of 200 metres. The density of fracturing is lower at deeper level but frequency is closely linked with the grade of hydrothermal activity. The chief fracture minerals include illite, kaolinite, unspecified mixed clay phases mainly illite, chlorite and smectite-group. The amount of iron sulphides is higher at the first 200 metres, where it often forms monomineralic coatings. The fracture plains are frequently covered by cohesive chlorite. Iron oxides and oxy-hydroxides occur in fractures at surficial zone, in core length 9.53 – 18.95 m., while graphite is present in several fractures in core length 20 - 50 m. Pervasive illitization concerns 11 % of the total core length and 36 % has calcite as major constituent in fracture fillings.

Kairanäytteen OL-KR22 JA OL-KR22B petrologia, petrofysiikka ja rakomineralogia

TIIVISTELMÄ

Tässä raportissa esitetään kairausnäytteitä OL-KR22 ja OL-KR22B koskevien tutkimusten tulokset. Kyseiset kairanreiät on tehty Olkiluodon tutkimusalueen kaakkois-osaan. Raportissa esitetään kairausnäytteen litologiaa sekä valittujen näytteiden koko-kiven kemiallista koostumusta, mineraalikoostumusta, tekstuuria ja petrofysikaalisia ominaisuuksia käsittelevien tutkimusten tulokset. Samoin kuvataan matalan lämpötilan raontäytemineraalit

Kairanreikä alkaa diateksiittisesta gneissijaksosta ja leikkaa aina 360 m:n pituudelle saakka varsin monotonisia diateksiittisia gneissejä, joita leikkaa pari leveää pegmatiittista graniittijuonta ja joissa on muutamia homogeenisia kiillegneisseistä ja mafisista gneisseistä koostuvia välikerroksia. Tämän alapuolella jatkuu aina 422 m:n kairaus-pituudelle saakka suonigneissijakso, jossa on kapeita kiillegneissivälikerroksia.

Yksityiskohtaiset petrologiset ominaisuudet on analysoitu 12 näytteestä. T-sarjaa edus-taa kuusi diateksiittista gneissinäytettä ja yksi suonigneissinäyte. Ainoastaan äärim-mäisen emäksiset ja happmat muunnokset puuttuvat tästä joukosta, jonka jäsenten SiO_2 vaihtelevat biotiittia paljon sisältävästä suonigneissistä analysoidusta 58 %:sta vaalean diateksiittisen gneissin 73 %:iin. Yksi mafinen gneissinäyte lukeutuu S-sarjaan. Se edustaa tämän ryhmän emäksisintä muunnosta ja sisältää $SiO2_2$:ta vain 43% mutta CaO:a siinä on noin 10%. P-sarjasta on valittu tutkittavaksi yksi TGG-gneissi, yksi diateksiittinen gneissi ja kaksi kiillegneissinäytettä. P-sarjalle tyypilliseen tapaan näytteiden fosforipitoisuus ylittää 0,4 % ilmoitettuna P_2O_5:na ja SiO_2–pitoisuus vaihtelee välillä 50 % ja 65 %.

Petrofysikaaliset ominaisuudet on määritetty 12 näytteestä. Mitatut parametrit ovat tiheys, magneettinen suskebtibiliteetti, luonnollinen remanentti magnetoituma, sähkö-vastus, P-aallon nopeus ja huokoisuus.

Kairausnäytteen OL-KR22 rakotiheys on keskimäärin 3,8 rakoa/metri. Rakoilu on voimakkaampaa 200 metrin kairauspituudelle saakka, jota syvempänä rakoilu keskittyy hydrotermisen muuttumisen läpikäyneisiin vyöhykkeisiin ja muihin rikkonaisuus-vyöhykkeisiin. Näissä vyöhykkeissä rakotäytteinä esiintyy illiittiä, kaoliniittia, erikseen määrittelemättömiä useamman savispesieksen muodostamia savisseostäytteitä (pää-asiassa illiitti, kloriitti ja smektiitti-ryhmä), rautasulfideja ja kalsiittia. Kloriitti muodos-taa tyypillisesti rakojen pinnoille kiinteän katteen, joka on usein alustana muille rakotäytteille. Rautaoksideja ja –oksihydroksideja esiintyy useissa raoissa kairaus-pituusvälillä 9,53-18,95 m ja grafiittia välillä 20-50 m. Kairauslävistyksestä on 11 % läpikotaisesti illiittiytynyttä. Kalsiittivaltaisia täyteseurantoja esiintyy 36 %:ssa kairaus-näytteen koko pituudesta.

TABLE OF CONTENTS

1 INTRODUCTION

According to the Nuclear Energy Act, all nuclear waste generated in Finland must be handled, stored and permanently disposed of in Finland. The two nuclear power companies, Teollisuuden Voima Oy and Fortum Power and Heat Oy, are responsible for the safe management of the waste. The power companies have established a joint company, Posiva Oy, to implement the disposal programme for spent fuel, whilst other nuclear wastes are handled and disposed of by the power companies themselves.

The plans for the disposal of spent fuel are based on the KBS-3 concept, which was originally developed by the Swedish SKB. The spent fuel elements will be encapsulated in metal canisters and emplaced at a depth of several hundreds of meters.

At present Posiva has started the construction of an underground rock characterisation facility at Olkiluoto. The plan is that, on the basis of underground investigations and other work, Posiva will submit an application for a construction licence for the disposal facility in the early 2010s, with the aim of starting disposal operations in 2020.

As a part of these investigations, Posiva Oy continues detailed bedrock studies to get a more comprehensive conception of lithology and bedrock structure of the study site. As a part of that work, this report summarises the results obtained from petrological and petrophysical studies and fracture mineral loggings of drill cores OL-KR22 and OL-KR22B.

1.1 Location and General Geology of Olkiluoto

The Olkiluoto site is located in the SW Finland, western part of the Eurajoki municipal and belongs to the Paleoproterozoic Svecofennian domain ca. 1900 - 1800 million years in age (Korsman et al. 1997, Suominen et al. 1997, Veräjämäki 1998,). The bedrock is composed for the most part of various, high grade metamorphic supracrustal rocks (Fig. 1-1), the source materials of which are various epi- and pyroclastic sediments. In addition, leucocratic pegmatites have been met frequently and also some narrow mafic dykes cut the bedrock of Olkiluoto. The practice of naming the rock types follows the orders of Posiva Oy (Mattila 2006).

On the basis of the texture, migmatite structure and major mineral composition, the rocks of Olkiluoto fall into four main classes: 1) gneisses, 2) migmatitic gneisses, 3) TGG gneisses, and 4) pegmatitic granites (Kärki & Paulamäki 2006). In addition, narrow diabase dykes have been met sporadically.

Subdivision of the gneissic rocks has to be based on modal mineral composition. *Mica gneisses*, mica bearing *quartz gneisses* and hornblende or pyroxene bearing *mafic gneisses* are often banded but rather homogeneous types have also been met. Quartz gneisses are fine-grained, often homogeneous and typically poorly foliated rocks that contain more than 60% quartz and feldspars but 20% micas at most. They may contain some amphibole or pyroxene and garnet porphyroblasts are also typical for one subgroup. Mica rich metapelites are in most cases intensively migmatitized but

sporadically also fine- and medium-grained, weakly migmatized gneisses with less than 10 % leucosome material occur. The content of micas or their retrograde derivatives

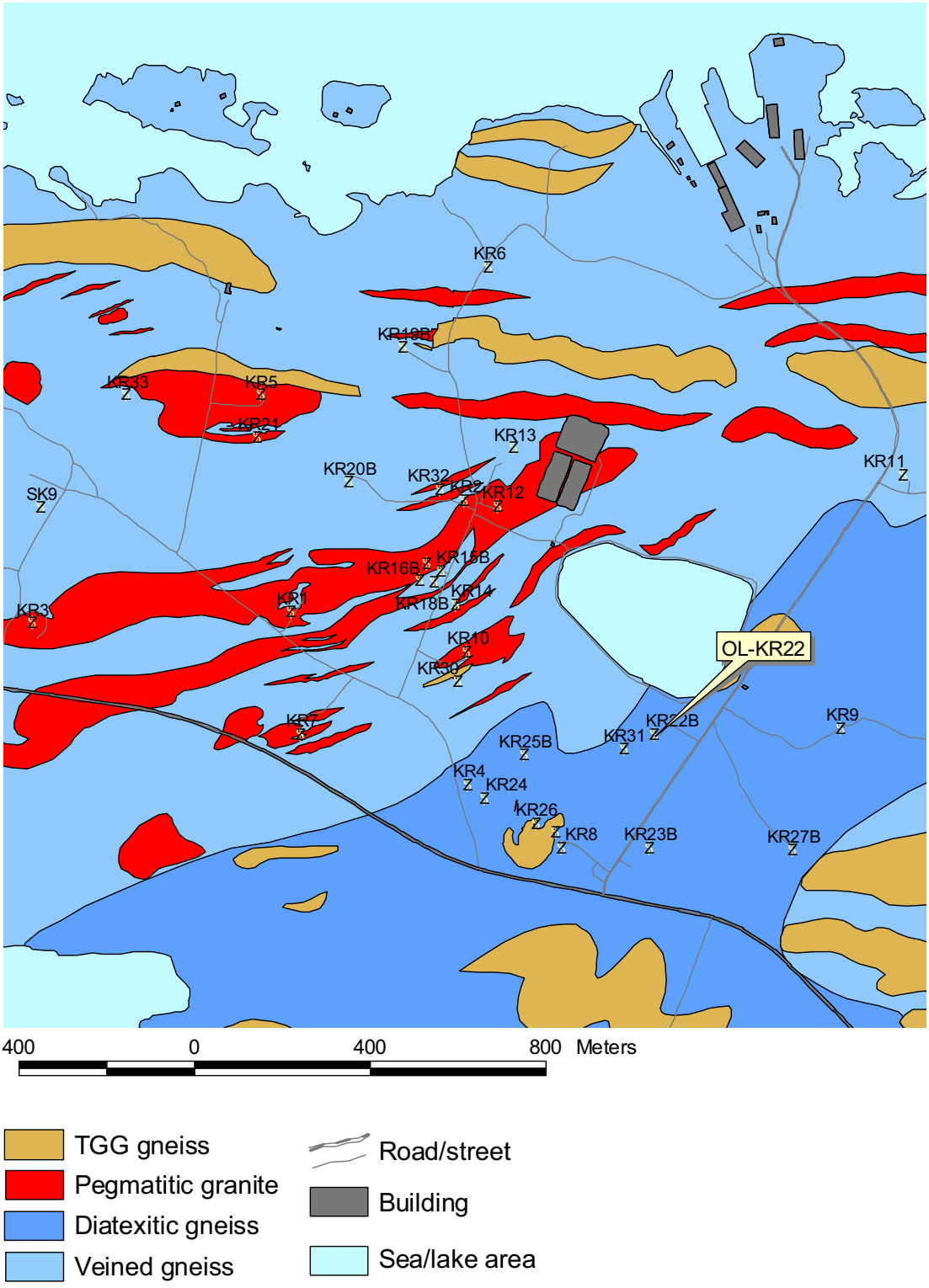

Figure 1-1. *General geology and location of bore hole starting points at Olkiluoto.*

exceeds 20% in these rocks. Cordierite or pinite porphyroblasts, typically 5 – 10 mm in diameter, are common constituents for one subgroup of mica rich rocks. Mafic gneisses and schists have been seen as different variants that have been called amphibolites, hornblende gneisses and chlorite schists. Certain, exceptional gneiss variants may contain in addition to dark mica and hornblende also some pyroxene or olivine.

Migmatitic gneisses have been defined as migmatites including more than 10% neosome. Ideal *veined gneisses* contain elongated leucosome veins the thicknesses of which vary typically from several millimetres to five – ten centimetres. The leucosome veins show a distinct lineation and appear as swellings of dykes or roundish quartz-feldspar aggregates that may compose augen-like structures the diameters of which vary between 1 and 5 cm. *Stromatic gneisses* represent a rather rare migmatite variety in Olkiluoto and the most characteristic feature of these migmatites is the existence of plane-like, linear leucosome dykes or "layers". Widths of these leucosome layers vary from several millimetres up to 10 – 20 cm. The paleosome is often well foliated and shows a distinct metamorphic banding or schistosity. The name *diatexitic gneiss* is used for other migmatite rocks that are more strongly migmatitized and show more wide variation in the properties of migmatite structures, which are generally asymmetric and disorganized. The borders of paleosome fragments or relicts of them are often ambiguous and they may be almost indistinguishable. This group includes migmatites that may contain more than 70% neosome and the paleosome particles of which are coincidental in shape and variable in size.

TGG gneisses are medium-grained, relatively homogeneous rocks which can show a weak metamorphic banding or blastomylonitic foliation but they can also resemble plutonic, not foliated rocks. One type of these gneisses resembles moderately foliated, red granites and one other grey, weakly foliated tonalites. In places, these rocks are well foliated, banded gneisses that show features typical for high grade fault rocks.

Pegmatitic granites are often leucocratic and very coarse-grained rocks. Sometimes large garnet and also tourmaline and cordierite grains of variable size occur in the pegmatitic granites. Mica gneiss inclusions and xenoliths are also typical constituents for wider pegmatite dykes.

On the basis of whole rock chemical composition these gneisses and migmatites can be divided into four distinct series or groups: T-series, S-series, P-series and mafic gneisses (Kärki & Paulamäki 2006). In addition to those, pegmatitic granites and diabases form their own groups which can be identified both macroscopically and chemically.

The members the T-series build up a transition series the end members of which are relatively dark and often cordierite bearing mica gneisses and migmatites which may have less than 60% SiO_2. Another end in this series is represented by quartz gneisses in which the content of SiO_2 exceeds 75%. These high grade metamorphic rocks have been assumed to originate from turbidite-type sedimentary materials and the end members of that series have been assumed to be developed from greywacke type, impure sandstones in other end and from clay mineral rich pelitic materials in other end of the series.

The members of the S-series have been assumed to originate from calcareous sedimentary materials or affected by some other processes that produced the final, skarn-type formations. The most essential difference between the members of the S-series and other groups is in the high calcium (>2% CaO) concentration of the S-type rocks. Relatively low contents of alkalis and high contents of manganese are also typical for this series. Various quartz gneisses, mica gneisses and mafic gneisses constitute the most typical members of the S series while migmatitic rocks are infrequent.

The P-series deviates from the others due to high contents of phosphorus. P_2O_5 content that exceeds 0.3% is characteristic for the members of the P-series whereas the other common supracrustal rock types in Olkiluoto contain typically less than 0.2% P_2O_5. Another characteristic feature for the members of the P-series is the comparatively high concentration of calcium which falls between the concentration levels of the T- and S-series. Mafic gneisses, mica gneisses, various migmatites and TGG gneisses are the most characteristic rock types of the P series. SiO_2 content of the mafic P-type gneisses varies between 42 and 52%, in the mica gneisses and migmatites it is limited between 55 and 65% and in the P-type TGG gneisses the variation is more wide the concentrations falling between 52 and 71%.

1.2 Boreholes and Drill Core Samples OL-KR22 and OL-KR22B

The starting points of the boreholes OL-KR22 and OL-KR22B are situated in the SE part of the Olkiluoto study site (Figure 1-1). The coordinates of the starting point of the borehole OL-KR22 are: X = 6792114.78, Y = 1526258.96 and Z = 7.40. Starting direction (azimuth angle) of the borehole is 271^o and its dip (inclination angle) is 59.1^o. The same values for the borehole OL-KR22B are: X = 6792119.05, Y = 1526259.03 and Z = 7.34. Starting direction (azimuth angle) is 270^o and its dip (inclination angle) is 60.0^o. Technical data dealing with the OL-KR22 and –KR22B drillings is represented by Niinimäki (2002).

1.3 The aim of this study and research methods

Hitherto, more than 40 deep bore holes have been drilled at the study site. The aim of this report is to represent the results of studies dealing with petrology, petrophysics and fracture minerals of the drill core samples OL-KR22 and OL-KR22B. A description of lithological units and their properties is presented in this report. Petrological properties such as whole rock chemical composition, mineral composition and microscopic texture of selected samples are described as well as the results of petrophysical measurements of the samples. Another aim was to map the locations and types of low temperature fracture infill minerals and, when necessary, to analyse and identify those.

Lithological mapping has been done by naked ayes utilizing the results of geophysical borehole measurements. Whole rock chemical analyses have been carried out in the SGS Minerals Services laboratory, Canada by X-ray fluorescence analyser (XRF), neutron activation analyser (NAA), inductively coupled plasma atomic emission

analyser (ICP), inductively coupled plasma mass spectrometer (ICPMS), sulphur and carbon analyser (LECO) and by using ion specific electrodes (ISE). The elements, methods of analysis and detection limits for individual elements have been represented in the Table 1-1. In addition, whole rock chemical composition of major elements is analysed at the department of Electron optics, University of Oulu by X-ray fluorescence analyser from 90 samples of the core OL-KR22 and from 10 samples of the core OL-KR22B.

Mineral compositions and textures of the selected samples have been determined by using Olympus BX60 polarization microscope equipped with reflecting and transmitting light accessories and a point counter.

Petrophysical measurements were carried out in the Laboratory of Petrophysics at the Geological Survey of Finland (GSF). Prior to the measurements, the samples were kept in a bath for 2.5 days using ordinary tap water (resistivity 50 – 60 ohmm). The parameters measured were density, magnetic susceptibility, natural remanet magnetization, electrical resistivity with three frequencies (0.1, 10 and 500 Hz), P-wave velocity and porosity.

Mapping of fracture infill minerals has been done by naked ayes utilizing stereomicroscopy when necessary. More detailed identification of mineral species of selected samples has been done by Siemens X-ray diffractometer at the department of electron optics, University of Oulu under control of O. Taikina-aho, FM.

1.4 Research Activities

Lithological logging and mapping of fracture infill minerals has been done by S. Gehör, PhD and A. Kärki, PhD during a mapping campaign on 28.7. – 1.8.2003 at the drill core archive of Posiva in Olkiluoto. During these studies Henri Kaikkonen and Pekka Kärki acted as research assistants and they also transcribed the dates collected during the studies. Engineer Tapio Lahdenperä is responsible for the checking and correcting the data files.

Drill core was sampled for studies of modal mineral composition, texture and whole rock chemical composition and in the latest stage also for measurements of petrophysical properties. The samples were selected by A. Kärki. Materials for detailed further studies have been selected on the basis of their frequency of appearance. Thus, the most common and typical rock types are represented roughly in the same proportion that they build up in the core sample. Polished thin sections have been prepared from these samples at the thin section laboratory of Department of Geosciences, University of Oulu for polarization microscope examinations.

The total number of prepared thin sections from the core OL-KR22 is 11 and 1 from the core OL-KR22B. Modal mineral compositions were determined by using a point counter and calculating 500 points per one sample. Aulis Kärki is responsible for microscope studies and also for description of petrography and handling of the results of the whole rock chemical analyses.

Table 1-1. *Elements, methods and detection limits for whole rock chemical analysis.*

Element	Method	Detection limit	Element	Method	Detection limit
SiO_2	XRF	0.01 %	Lu	ICPMS	0.05 ppm
Al_2O_3	XRF	0.01 %	Nb	ICPMS	1 ppm
CaO	XRF	0.01 %	Nd	ICPMS	0.1 ppm
MgO	XRF	0.01 %	Ni	ICPMS	5 ppm
Na_2O	XRF	0.01 %	Pr	ICPMS	0.05 ppm
K_2O	XRF	0.01 %	Rb	ICPMS	0.2 ppm
Fe_2O_3	XRF	0.01 %	Sm	ICPMS	0.1 ppm
MnO	XRF	0.01 %	Sn	ICPMS	1 ppm
TiO_2	XRF	0.01 %	Sr	ICPMS	0.1 ppm
P_2O_5	XRF	0.01 %	Ta	ICPMS	0.5 ppm
Cr_2O_3	XRF	0.01 %	Tb	ICPMS	0.05 ppm
LOI	XRF	0.01 %	Tm	ICPMS	0.05 ppm
Mn	ICP	2 ppm	U	ICPMS	0.05 ppm
Ba	ICPMS	0.5 ppm	W	ICPMS	1 ppm
Ce	ICPMS	0.1 ppm	Y	ICPMS	0.5 ppm
Co	ICPMS	10 ppm	Yb	ICPMS	0.1 ppm
Cu	ICPMS	10 ppm	Zn	ICPMS	5 ppm
Cr	ICPMS	10 ppm	Zr	ICPMS	0.5 ppm
Cs	ICPMS	0.1 ppm	Cl	ISE	50 ppm
Dy	ICPMS	0.05 ppm	F	ISE	20 ppm
Er	ICPMS	0.05 ppm	C	LECO	0.01 %
Eu	ICPMS	0.05 ppm	S	LECO	0.01 %
Gd	ICPMS	0.05 ppm	Br	NAA	0.5 ppm
Hf	ICPMS	1 ppm	Cs	NAA	0.5 ppm
Ho	ICPMS	0.05 ppm	Th	NAA	0.2 ppm
La	ICPMS	0.1 ppm	U	NAA	0.2 ppm

Petrophysical properties have been measured at the Geological Survey of Finland from the same samples that have been selected for petrological studies. Markku Paananen, Lic. Tech. from the GSF is responsible for handling and description of petrophysical data.

S. Gehör carried out the handling of fracture mineral data and he is also responsible for the selection of fracture mineral materials for further studies. S. Gehör also composed the section dealing with the fracture minerals.

2 PETROLOGY

The practice for naming (Mattila 2006) and lithological classification proposed by Kärki and Paulamäki (2006) has been utilized in the description and grouping of lithological units. More detailed classification has to be based on the evaluation of whole rock chemical composition or modal mineral composition and that is not possible without information based on the accurate results of instrumental analysis.

2.1 Lithology

The drill holes intersect down to length of 360 m a rather monotonous diatexitic gneiss unit which is intruded by a couple of rather wide pegmatitic granite dykes and has several homogeneous mica gneiss and mafic gneiss subsections. Below that, down to the drilling length of 422 m a fluctuating section of veined gneisses with narrow mica gneiss interbeds is located. The lowermost part of the core sample is composed of rather homogeneous mica gneisses with various migmatite subsections (Figure 2-1). A more detailed description of lithological units is presented in the Tables 2-1 and 2-2.

Table 2-1. *Lithology of the drill core sample OL-KR22.*

Drilling length (m)	Lithology
40.66 – 46.00	PEGMATITIC GRANITE – DIATEXITIC GNEISS mixture which is irregular, breccia-like for a part and in which the components fluctuate randomly. The proportion of granitoids material is 50% in average.
46.00 – 46.27	Crushed migmatite.
46.27 – 52.20	VEINED GNEISS – DIATEXITIC GNEISS mixture. Veined gneisses with a large proportion of leucosome dominate in the upper part of the section but in the deeper part the rock changes to breccia-like rock which is subsequently crushed. The rock contains ca. 40% leucosome.
52.20 – 53.60	PEGMATITIC GRANITE which is, for a part, leucocratic and coarse-grained pegmatite but for a part it is build of irregular, brecciated mixture of gneisses and pegmatites. Gneiss blocks compose ca. 30% of the whole rock volume.
53.60 – 56.35	DIATEXITIC GNEISS – QUARTZ GNEISS – PEGMATITIC GRANITE mixture in which various components of different sizes and shapes fluctuate randomly. The rock mixture has features of intrusive breccia and is strongly altered in the whole section. The proportion of granitoid component is ca. 50%.
56.35 – 58.15	MAFIC GNEISS or fine-grained and relatively homogeneous amphibolite which seems to be strongly chloritized and saussuritized.

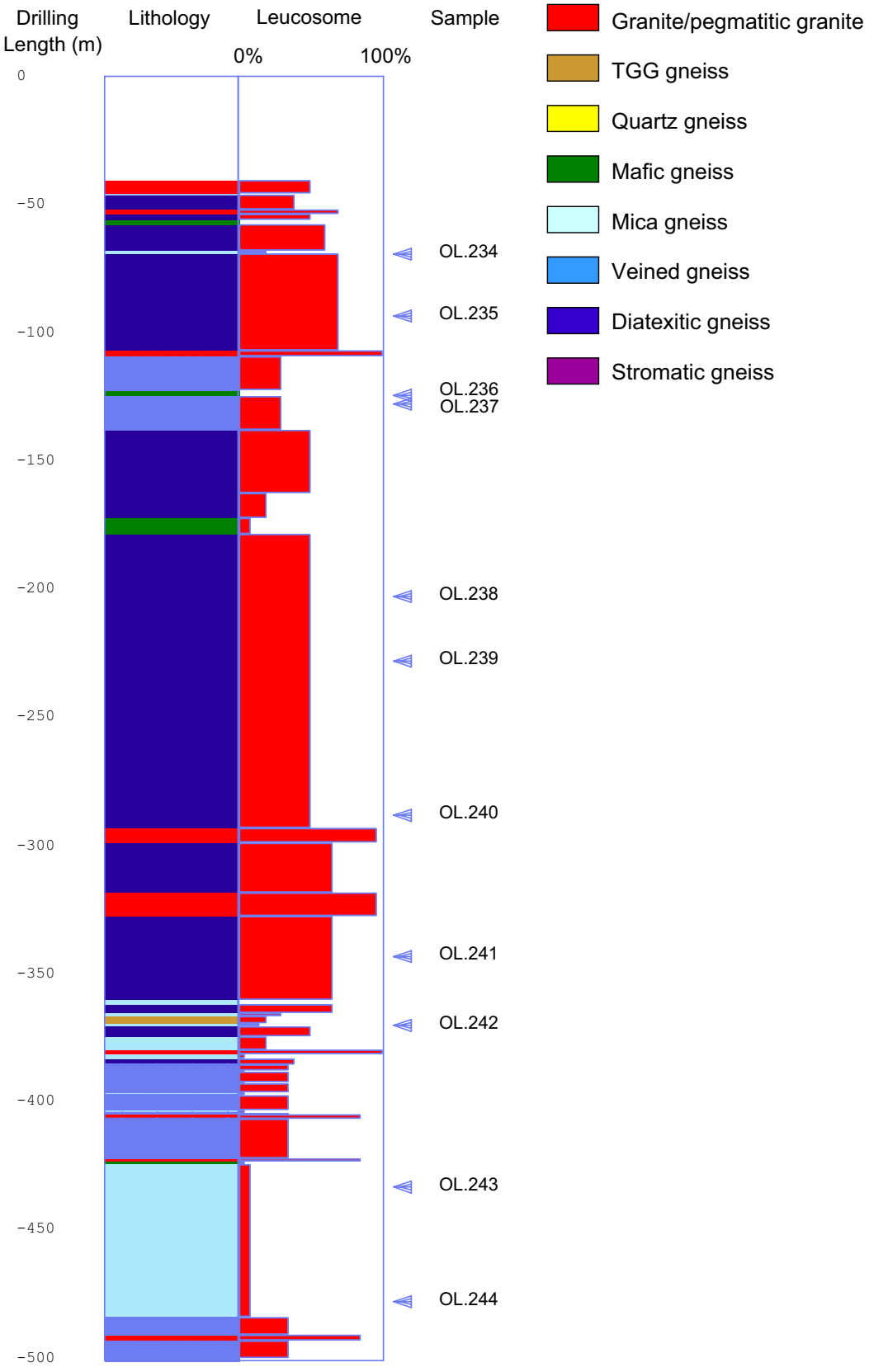

Figure 2-1. *Lithology, leucosome + pegmatite material percentage (= leucosome) and sample locations, drill core OL-KR22.*

58.15 – 67.90	DIATEXITIC GNEISS which, for a part, resembles the veined gneisses but, for a part, is a totally irregular diatexite in which the proportion of leucosome is ca. 60%.
67.90 – 69.22	QUARTZ GNEISS – MICA GNEISS mixture in which the gneisses are homogeneous, weakly foliated and contain ca. 20% leucosome. Granite pegmatites intersect the gneisses as 10 – 20 cm wide and randomly situated dykes.
69.22 – 107.00	DIATEXITIC GNEISS which contains cordierite and high proportion, close to 70% leucosome and pegmatite dykes. A small part of paleosome is composed of quartz gneiss and those sections are close to free of leucosome while typical, biotite rich sections are strongly migmatitized and also intruded by 20 – 80 cm wide pegmatitic dykes.
107.00 – 109.25	PEGMATITIC GRANITE which is coarse-grained, leucocratic and epidotized in places but rather free of gneiss inclusions.
109.25 - 122.80	VEINED GNEISS in which the leucosome veins are 1 – 3 cm in width and in addition to that, the rock is intruded by 10 – 60 cm wide pegmatite dykes. The paleosome is medium-grained and shows a distinct metamorphic banding.
122.80 - 125.05	MAFIC GNEISS (amphibolite/chlorite schist) which is homogeneous and fine to medium-grained.
125.05 - 138.20	VEINED GNEISS in which leucosomes are 1 – 3 cm wide veins and, in addition to those, the rock is intruded by 10 – 60 cm wide pegmatite dykes. The paleosome is medium-grained and shows a distinct metamorphic banding.
138.20 - 162.98	DIATEXITIC GNEISS in which the migmatite structure is highly variable. A part of the section resembles vein migmatites but mostly it is composed of irregular diatexite in which gneiss inclusions of various sizes are typical.
162.98 - 172.40	DIATEXITIC GNEISS – MICA GNEISS mixture the paleosome of varies from homogeneous quartz gneisses to banded mica gneisses. In the upper part of the section, until the drilling length of 165.70 m the proportion of leucosome is large but from that point onward leucosome composes 20% of the rock volume and its type of occurrence is highly variable.
172.40 - 178.55	MAFIC GNEISS (amphibolite) which is fine- or medium-grained, rather homogeneous and, in particular in the end of the section, contains ca 10% pegmatitic granite veins which are 20 – 50 cm in thickness.

178.55 – 293.40 DIATEXITIC GNEISS which resembles veined gneisses, for a part, but mostly it is coarse-grained and the contacts between leucosome and paleosome are diffuse and irregular. At the drilling length of 220 m the rock transforms to TGG gneiss-like, more homogeneous gneiss type and at the drilling length of 235 m again to diatexite which contains vein migmatite-like subsections. The proportion of leucosome is 50% in average.

293.40 – 299.00 PEGMATITIC GRANITE which is coarse grained and contains dark grains with diameter ranging from 5 to 10 mm. The pegmatite contains ca. 5% small gneiss inclusions and biotite schlieren.

299.00 – 318.40 DIATEXITIC GNEISS which is medium-grained and contains 60 - 70% leucosome in average.

318.40 – 327.75 PEGMATITIC GRANITE which is coarse-grained, leucocratic and contains randomly situated, 5 – 10 cm wide mica schlieren ca. 5%.

327.75 – 360.20 DIATEXITIC GNEISS the paleosome of which is medium-grained. The leucosome is porphyritic for a part and composes 60-70% of the rock volume. In addition, the migmatite is intruded by 20 – 80 cm wide pegmatitic granite dykes.

360.20 – 362.10 MICA GNEISS which is medium-grained, homogeneous and, for a part, amphibole bearing. The gneiss contains 1 – 2% leucosome.

362.10 – 365.30 DIATEXITIC GNEISS in which the proportion of leucosome is ca. 65%.

365.30 – 366.85 MICA GNEISS which is fine- or medium-grained and contains ca. 30% leucosome.

366.85 – 369.25 TGG GNEISS which is medium-grained, weakly banded and contains ca. 20% leucosome-like dykes.

369.25 – 370.50 MICA GNEISS which is medium-grained and homogeneous.

370.50 – 374.95 DIATEXITIC GNEISS in which one, 0.5 m wide homogeneous mica gneiss layer occur and which is intruded by 15 – 60 cm wide pegmatite dykes.

374.95 – 379.90 MICA GNEISS which is medium-grained, homogeneous and contains ca. 10% leucosome. In addition, the rock is intruded by several, rather wide pegmatitic granite dykes.

379.90 – 381.30 PEGMATITIC GRANITE which is free of inclusions.

381.30 – 383.25 MICA GNEISS which is medium-grained and homogeneous. The rock contains ca. 5% leucosome and narrow pegmatite dykes situated randomly in the section.

383.25 – 385.40 DIATEXITIC GNEISS which contains 40% leucosome.

385.40 – 385.85 MAFIC GNEISS.

385.85 – 405.30 VEINED GNEISS in which the paleosome is mostly medium-grained and biotite bearing but in subsections 388.00 m – 388.50 m, 392.20 m – 392.90 m, 396.30 m – 397.40 m and 403.40 m – 404.20 m the paleosome is homogeneous and medium-grained mica gneiss or mafic gneiss. In the vein migmatite average proportion of leucosome is 35%.

405.30 – 406.50 PEGMATITIC GRANITE.

406.50 – 422.50 VEINED GNEISS in which subsections of irregular diatexites and homogeneous mica gneiss occur. The average proportion of leucosome is 35%.

422.50 – 423.30 PEGMATITIC GRANITE.

423.30 – 424.50 MAFIC GNEISS – MICA GNEISS mixture in which the proportion of leucosome is 5%.

424.50 – 483.96 MICA GNEISS – DIATEXITIC GNEISS mixture which contains 10 – 30% leucosome in average and, in general, the rock is relatively homogeneous but intruded by 5 – 30 cm wide pegmatitic granite dykes.

483.96 – 490.90 VEINED GNEISS which, in places, has typical veined structure but resembles in places irregular diatexites and elsewhere homogeneous mica gneisses. The average proportion of leucosome is 35%.

490.90 – 493.20 PEGMATITIC GRANITE which is coarse-grained and leucocratic.

493.20 – 500.47 VEINED GNEISS.

Table 2-2*. Lithology of the drill core sample OL-KR22B.*

Drilling length (m)	Lithology
8.15 – 20.75	DIATEXITIC GNEISS which is pervasively strongly altered, reddish and hematite bearing for a part and greenish for a part. The proportion of leucosome is 70 – 80%.

20.75 – 27.80 DIATEXITIC GNEISS in which the migmatite structure and leucosome bodies are totally irregular and the contacts between different components are diffuse. The subsection from 24.60 m to 25.25 m is composed of homogeneous, fine-grained mafic gneiss in which narrow breccia zones, 5 – 10 cm in thickness, occur. The proportion of leucosome is large, 70 – 80%.

27.80 – 32.50 TGG GNEISS which is medium-grained and relatively weakly oriented. The rock contains ca. 10% leucosome.

32.50 – 45.55 DIATEXITIC GNEISS in which narrow subsections of veined gneisses occur. The most part of the section is composed of irregular diatexite in which the proportion of leucosome is 70 - 80%.

2.2 Whole Rock Chemistry

Whole rock chemical composition is analysed from 12 samples. Seven of those are migmatites of the T series, four are gneisses and migmatites of the P series and one is mafic, S-type gneiss. The numerical results of the whole rock chemical analyses are represented in the Appendix 1. In addition, 100 XRF major element analyses were made from samples that were taken by 5 m average interval from the core sample. The results of these analyses are given in the Appendix 2. The aim of these extra analyses was to clarify the ideas of distribution and proportions of members of various rock series (T, S and P series).

The T series is represented by six diatexitic gneiss samples and one veined gneiss sample which give an extensive overview of the whole series. Only the extremely basic and acidic types are excluded. SiO_2 concentration varies from 58% analysed from a biotite rich veined gneiss to ca. 73% analysed from a light diatexitic gneiss (Fig. 2.2). Following the increase in silicity the content of TiO_2 decreases from 1% to 0.2%, Al_2O_3 from 18% to 14%, Fe_2O_3 from 8% to 2% and MgO from 4% to 1% in various migmatite samples. The contents of CaO and Na_2O seem to have increasing trends. CaO concentration increases from 0.5% to 1.5% and Na_2O from 1.5% to 3.5% while SiO_2 increases from 58% to 72% (Appendix1).

Trace element concentrations and element ratios are in the most cases quite typical for the T series (Fig. 2.3). The only exception can be seen in the REE diagram which depicts the sample OL.235. In that the REE concentrations are systematically lower than in other samples and it also shows a negative Eu anomaly. However, the other trace element concentrations are strictly in the anticipated numbers. Only the contents of Th, Ce and Sm are in the sample 235 a little lower than typical numbers (Fig. 2.3).

One mafic gneiss sample is included into the S-series. The sample is the most mafic example analysed from this group. It contains SiO_2 only 43% and CaO ca. 10% and, in other respects, it is a typical mafic gneiss of the S series including 12% Al_2O_3, 13% Fe_2O_3 and 16% MgO. The contents of alkalis are low, below 1% both Na_2O and K_2O.

The REE and other trace element concentrations are typical for mafic S-type gneisses but deviate slightly from the other groups. The gently dipping REE diagram and total lack of europium anomaly (Fig. 2.3) demonstrate this difference.

The P series is represented by one TGG gneiss, one diatexitic gneiss and two mica gneiss samples. Content of phosphorus exceeds 0.4%, given as P_2O_5, in every of those. The content of aluminium is constantly ca. 17% despite of the change in silicity (Fig. 2-2). The other major element concentrations show a clear decreasing trend which is directly controlled by the increase in silicity (Fig. 2-2). Migmatites are not numerous in the P series and only four samples of those are of diatexitic type. Major element concentrations in those as well as in the sample analysed now fall to the numbers typical for the P-type gneisses (Fig. 2-2). The concentration of potassium is the only exception and K_2O concentration which exceeds 3% (Appendix 1) is similar to that of the P type TGG gneisses. Equally, the contents of light REE´s (Fig. 2-3) are lower and end element ratios different (gently dipping REE pattern) from those typical for less migmatitic members of the P series. Anyhow, the other trace element concentrations do not deviate remarkably from typical concentrations (Fig. 2-3).

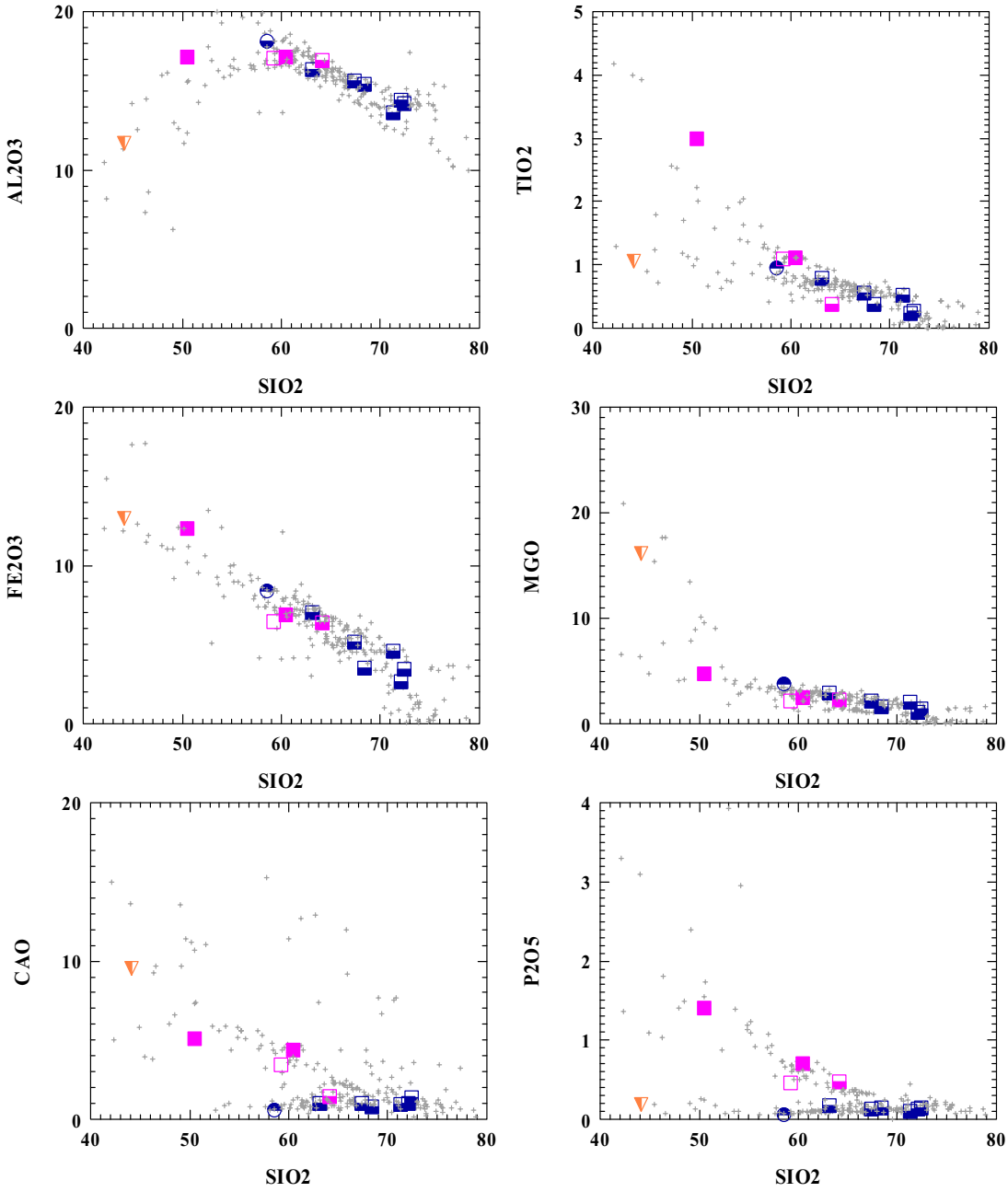

Symbols: ▼ = mafic gneiss (S- or P-series), ◒ = veined gneiss, ◧ = diatexitic gneiss, ■ = mica gneiss, ◆ = quartz gneiss, □ = TGG gneiss, ▲ diabase, ▲ = mafic metavolcanic rock and ● = pegmatitic granite from the drill core OL-KR22. + = sample from some other drill core.
Explanation for the colours: blue = T-series, orange = S-series, violet = P-series, red = granite, green = mafic metavolcanic rock and black = diabase.

Figure 2-2. *Chemical variation diagrams, Harker diagrams (weight percentage values) for the rocks of the drill core sample OL-KR22.*

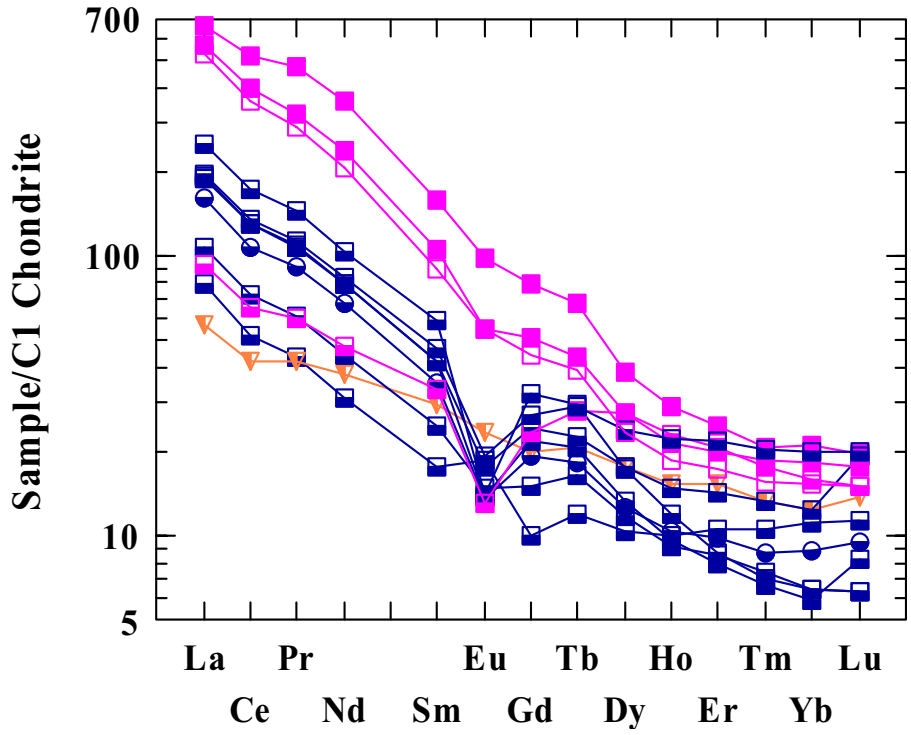

A.

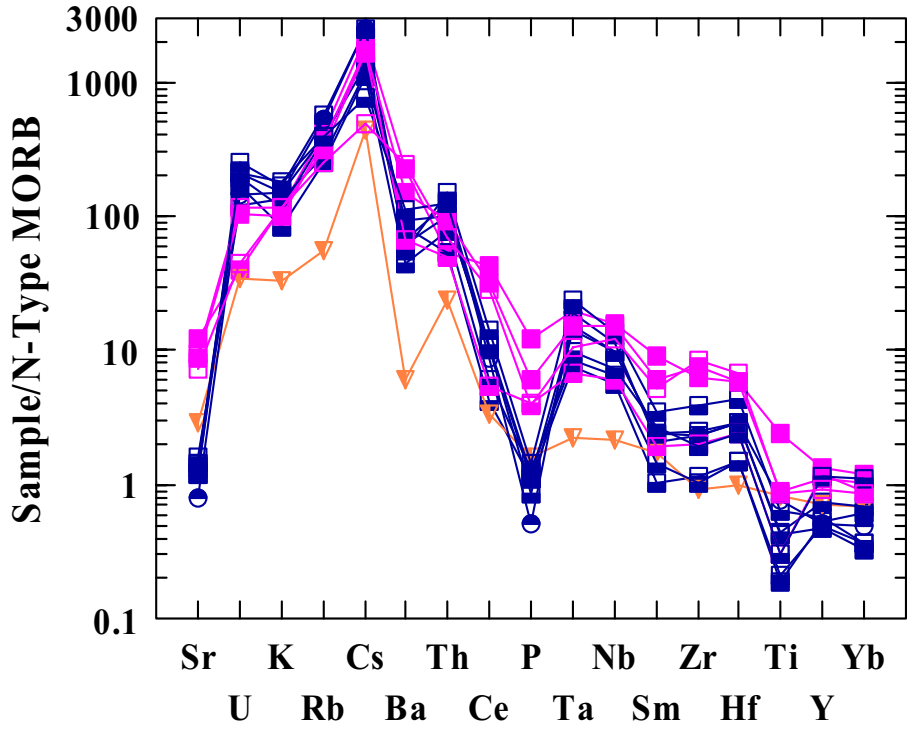

B.

Figure 2-3 A. *Multielement diagram and* ***B.*** *REE-diagram showing the enrichment factors for the samples from the drill core OL-KR22. Symbols as in the Fig. 2-2.*

The TGG gneiss sample contains less than 60% SiO_2 and thus it belongs to the subgroup of less silicic variants in the P series. P_2O_5 concentration is ca.0.45% and CaO concentration exceeds 3% which are typical numbers for the P type gneisses. Similarly, the high content of aluminium and moderate contents of titanium and iron (Fig. 2-2) are typical in that sequence. The REE pattern is identical to that of the mica gneiss sample and the same similarity is visible in the other trace element concentrations (Fig. 2-3).

The samples 234 and 242 represent both extremities in the sequence of the P type mica gneisses. SiO_2 concentration of the former is ca. 50% and of the latter ca. 60%. P_2O_5 concentration decreases from 1.4% to 0.7% and CaO from 5% close to 4% as silicity increases (Fig. 2-2). Other major element concentrations are strictly in the anticipated numbers, too. REE patterns (Fig. 2-3) are typical for the P series and the REE concentrations are systematically higher in the less silicic sample than in the silicic one. The other trace element concentrations are also typical for the P series (Fig. 2-3) even though the silicic sample is enriched in U, Th and Zr in comparison to the less silicic one.

The results of the additional, 100 major element analyses are represented in the Appendix 2. The chemical border between T and P series is set at the 0.2% content of P_2O_5. The border between the members of the T and S series is set at the 2% content of CaO. According to this testing, the members of the P and T series are located at all depths in the drill hole (Fig. 2-4). The lengths of subsections where P-type gneisses dominate vary from a couple metres to 25 metres. The pure T-type gneiss sections vary from 10 to 50 m in length. The T-type gneisses compose ca. 71% and P-type gneisses 20% of the total length of drilling section composed of supracrustal materials. S-type gneisses compose the remaining 9% and those are located in subsections located between drilling lengths of 120 and 140 m and in three subsections below drilling length of 370 m (Fig. 2-4).

The average distance between individual points of analysis is 4.88 m. This length is rather long when compared to original thicknesses of turbidite type sedimentary layers which may vary from centimetres to several tens of metres. Thus the exact proportions and distribution of the members of these three rock classes are not possible to detect on the basis of this test material. This is visible in the result material and also in the chemical diagrams (Fig. 2-4) due to coincidental fluctuation element concentrations. In the primary materials the changes of compositions are gradational and the same gradational changes should be visible in the transition of types and compositions of present migmatite materials. If information of real distribution is needed, the interval between analysis points should be evidently shorter than thicknesses of original sedimentary beds. However, this result augments the view of proportions of P-type S-type and T-type gneisses at the study site. The members of the T series seem to compose 70%, members of the P series 20% and members of the S series the remaining 10% in the bedrock volume intersected by the drill hole OL-KR22.

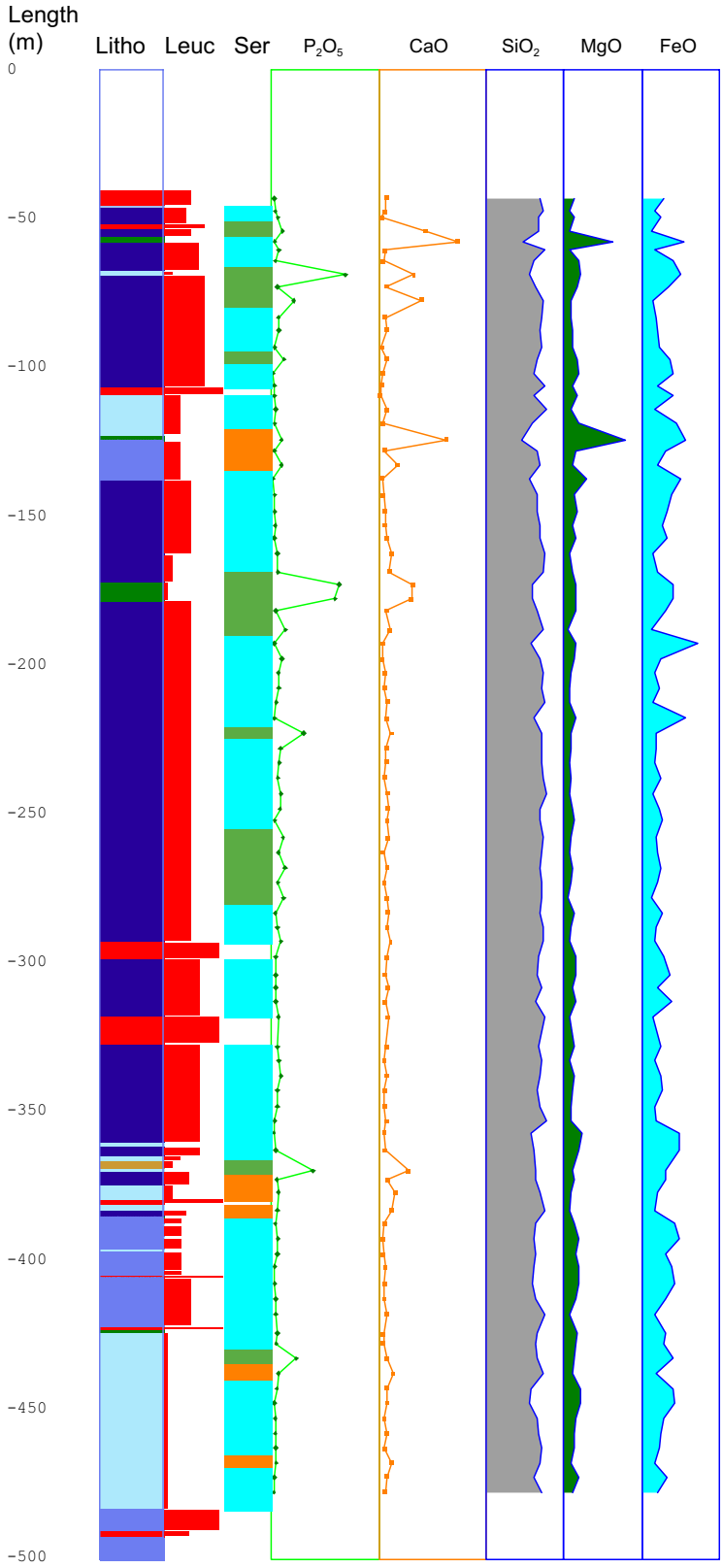

Figure 2-1. *Lithology (Litho, explanations as in the Fig. 2-1), Leuc = leucosome + pegmatite material percentage, scale 0 – 100%, rock series; blue = T series, green = S-series, green = S-series and certain element concentrations, drill core OL-KR22. Scales of element concentration diagrams: P_2O_5 = 0 – 2%, CaO = 0 – 16%, SiO_2 = 0 - 100%, MgO = 0 – 20% and FeO = 0 – 20%..*

2.3 Petrography

The drill core KR22 is represented by 12 samples of which 8 belong to the T series, 1 to the S series and four to the P series. Modal mineral compositions of these samples are represented in the Appendix 3.

T- Series

The diatexitic T-type gneisses are represented by six samples, 235, 237, 238, 239, 240, 241 and 244, which belong to the more acidic half of the whole series. SiO_2 varies between 63 and 73% in these diatexites. The content of quartz varies between 27% and 43%, content of plagioclase between 11% and 27% and K-feldspar typically between 11 and 25%. The proportion of biotite or total number of biotite and chlorite, if the latter is present, varies between 10 and 25%. In general, more silicic varieties are richer in felsic minerals and poorer in mafic ones, but the ratio is not linear and distinct. Cordierite has been present in every sample but now it is pinitic for the most part. Sillimanite belongs to the assemblage as a minor component. The samples 235 and 244 contain hematite and pyrite as the only opaques while the others include pyrrhotite, pyrite and chalcopyrite with certain rare phases of sulphide minerals.

The diatexitic gneisses are rather coarse-grained and poorly foliated. Features of rough metamorphic banding can be imagined but the dark bands are more or less irregular, 2 – 4 mm wide zones into which the mafic minerals are concentrated. Preferred orientation of micas within these zones is not always well developed and the mica scales are 1 – 2 mm long, at most. Leucocratic parts in the diatexites are medium-grained and granoblastic. Diameters of typical feldspar and quartz grains are ca. 2 mm and they compose totally irregular shaped, often roundish grains which have somehow interfingered contacts bulged against to each other. The diatexitic samples demonstrate a moderate degree of alteration by containing totally pinitized cordierite, slightly chloritized biotite and partially saussuritized plagioclase.

The veined gneiss sample (230) of the T series is less silicic than any of the diatexites. SiO_2 concentration of 59% is rather low number among the whole T series, too. The gneiss is evidently darker and contains ca. 40% biotite. Quartz content is 22%, plagioclase 12% and K-feldspar 10% which are typical concentrations for this kind of T-type rocks. 10% content of pinite and small amount of sillimanite are also typical numbers. Similarly, a small content of pyrrhotite, chalcopyrite and hematite is typical for this rock type. The veined gneiss is relatively coarse-grained and metamorphic banding in the paleosome of it is well developed. Mica scales are approximately 1 mm long and perfectly concentrated into the dark bands which are 2 -3 mm wide. Dark bands are wavy and border the leucocratic parts or veins. Leucocratic veins are medium-grained and granoblastic. Feldspar and quartz grains are irregular shaped and their diameter is 1 mm, in average. The veined gneiss sample demonstrates moderate degree of alteration like the diatexitic samples of this series.

S-series

The Mafic S-type gneiss (236) is the only representative in this category. It is composed near to completely of hornblende the proportion of which is 82%. Biotite composes 10% and chlorite 5%. In addition, the sample contains only a trace amount of plagioclase and apatite. Opaque minerals count 0.6% of the rock volume and magnetite, pyrite, pyrrhotite and chalcopyrite are the most common species.

The mafic gneiss is medium-grained with average diameter of amphibole grains close to 2 mm. Due to large proportion of amphibole the gneiss should have nematoblastic texture but the amphibole grains are roundish and their contacts are interfingered with each other. Thus, the texture resembles granoblastic texture of felsic, medium-grained gneisses. The gneiss is not foliated and no indication of preferred orientation of any mineral is detectable. Mica and chlorite scales are located randomly into the amphibole mass and also their orientation is random. Amphibole of the rock does not show any features of secondary alteration but biotite is chloritized for a part.

P-series

The P series is represented by one diatexitic gneiss sample, two mica gneisses and one TGG gneiss sample.

The T-type diatexitic gneiss (sample 243) belongs to an infrequent subgroup in the P series as the total number of samples studied in detail from this category is only 5. The sample studied now includes 64% SiO_2 and is the most silicic variety analyzed until now. Quartz content of 36%, plagioclase of 11%, K-feldspar of 19% and biotite of 5% are not anomalous numbers for the P-type migmatites. On the contrary, rather high content of muscovite (8%) is not very typical but within the leucosome material it has been seen also earlier. Similarly, high content of cordierite is atypical for P-type rocks but in migmatitic varieties that species has been detected also in the other samples. Typical opaques are pyrrhotite, hematite and chalcopyrite.

This gneiss is medium-grained, granoblastic and the paleosome of it is not evidently foliated. Quartz, feldspar and primary cordierite grains are equidimensional and more or less roundish. Mafic minerals are concentrated into the mass that may borders 5 – 10 mm wide, roundish quartz-feldspar aggregates or patches making the whole structure similar to certain porphyry-like rocks elsewhere in the study area. The sample shows features of moderate degree of alteration. Cordierite is totally pinitized, plagioclase is slightly saussuritized but the other minerals are rather fresh.

The mica gneisses of the P series selected for the detailed studies represent both ends in that sequence. The sample 234 includes SiO_2 only 50.5% which is the lowest number analyzed and the other sample (242) contains 60.5% SiO_2 which is one of the highest values in this category. Quartz contents are 26% and 30%, plagioclase contents 27% and 36%, and biotite contents 36% and 28% in the less silicic and more silicic sample, respectively. Rather high content of apatite, ca. 2% is typical for this kind of rocks in the P series. Similarly the total lack of K-feldspar is typical for non-migmatitic

members of this sequence. Opaques compose of magnetite, ilmenite, pyrrhotite, pyrite and chalcopyrite.

The mica gneisses are fine-grained and poorly foliated. The mica scales are 0.5 mm long in average and their orientation is random. Quartz and plagioclase grains are equidimensional, often somehow roundish and their average diameter is 0.5 mm. Orientation of mica scales is random and the scales are surrounded by granoblastic quartz-feldspar mass making the whole structure resemble the granoblastic structure of mica bearing quartzites. Features of weak foliation and metamorphic banding can be imagined but those are not obvious. The degree of secondary alteration of these samples is low as only a small part of biotite is chloritized and plagioclase is slightly pigmented by fine-grained saussurite.

The P-type TGG gneiss sample (245) includes 59% SiO_2 and thus it belongs to the less silicic half in the sequence. Quartz content of 14% is typical value for this type rocks. 27% content of plagioclase and 5% both K-feldspar and biotite are low numbers for this sequence but those will be explained by high contents of chlorite (15%) and saussurite (30%). A couple percent content of apatite and sphene are typical for this kind of TGG gneisses. Similarly, pyrrhotite, pyrite and chalcopyrite are typical sulphide phases.

The gneiss is granoblastic and medium-grained. Quartz-feldspar aggregates with diameters varying from 5 to 10 mm are typical elements for these gneisses. These aggregates or patches are situated into a more mafic “groundmass” which contains most part of the micas. Typical diameters of roundish felsic mineral grains vary between 1 and 2 mm while the biotite scales are 0.5 mm long, at most. Segregation of mafic and felsic minerals is not perfect and the foliation is poorly developed. This increases markedly the isotropy of physical properties of these rocks. The sample studied here shows features of strong secondary alteration. Large part of biotite is chloritized and plagioclase is almost pervasively pigmented by microcrystalline saussurite. The saussurite proportion of 30% is exceptional large.

3 PETROPHYSICS

For the petrophysical measurements, the samples were sawn flat, the length of the samples being typically 5 – 6 cm. The measurements were carried out in the Laboratory of Petrophysics at the Geological Survey of Finland. Prior to the measurements, the samples were kept in a bath for 2.5 days using ordinary tap water (resistivity 50 – 60 ohmm). The parameters measured were density, magnetic susceptibility, natural remanet magnetization and its orientation, electrical resistivity with three frequencies (0.1, 10 and 500 Hz), P-wave velocity and porosity.

Densities were determined by weighing the samples in air and water and by calculating the dry bulk density. The reading accuracy of the balance used is 0.01 g and the repeatability for average-size (200 cm^3) hand specimens is 2 kg/m^3.

Porosities were determined by the water saturation method: the water-saturated samples were weighed before and after drying in an oven (three days in 105 °C). The reading accuracy of the balance used for porosity measurements is 0.01 g. The effective porosity is calculated as follows:

$$P=100 \cdot (Mwa - Mda)/ (Mwa - Mww) \quad (1)$$

where Mda = weight of dry sample, weighing in air
Mwa = weight of water-saturated sample, weighing in air
Mww = weight of water-saturated sample, weighing in water
P = porosity.

The magnetic susceptibility was measured with low-frequency (1025 Hz) AC-bridges, which are composed of two coils and two resistors. Standard error of the mean for repeated measurements is c. $10 \cdot 10^{-6}$ SI.

The remanent magnetization was measured with fluxgate magnetometers inside magnetic shielding. For repeated measurements, the standard error of the mean is c. $10 \cdot 10^{-3}$ A/m.

The specific resistivity was determined by a galvanic method using the MAFRIP equipment, constructed at the Geological Survey of Finland. Used frequencies were 0.1, 10 and 500 Hz, allowing also the determination of induced polarization (IP). The measuring error is less than 2 % within the resistivity range of 0.1 – 100000 ohmm.

To determine the P-wave velocity, the length of the sample and the propagation time through the sample must be known. An electronic pulse was produced by a pulse-generator, and the propagation time was measured using echo-sounding elements and an oscilloscope.

The petrophysical parameters measured are presented in a table in the Appendix 4.

3.1 Density and magnetic properties

Variation in density and magnetic properties in crystalline rocks are dominated mainly by their mineralogical composition, however porosity may have a slight effect in density. The measured density values for these 12 samples range between 2658 and 3085 kg/m^3. The highest value is measured from sample 236, which is mafic gneiss. From the rock types, diatexite samples appear to be lighter than the other samples.

Most of the samples are paramagnetic or weakly ferrimagnetic with susceptibility values ranging from $130 \cdot 10^{-6}$ SI to $3780 \cdot 10^{-6}$ SI. In Fig. 3-1a, susceptibility vs. density of the measured samples is shown. For comparison, the data previously measured from deep boreholes OL-KR1 – OL-KR6, minidrill holes and shallow boreholes are shown in Fig. 3-1b. Most of the samples measured correspond rather well with the paramagnetic mica gneiss population of the older data. There are two slightly ferrimagnetic samples, number 243 (P series TGG gneiss) and 234 (P series mica gneiss), indicating small amounts of ferrimagnetic minerals.

a)

Data: Borehole KR22

b)

Data: Boreholes KR1 - KR6
Minidrill samples from outcrops and investigation trenches
Shallow boreholes (POKA)

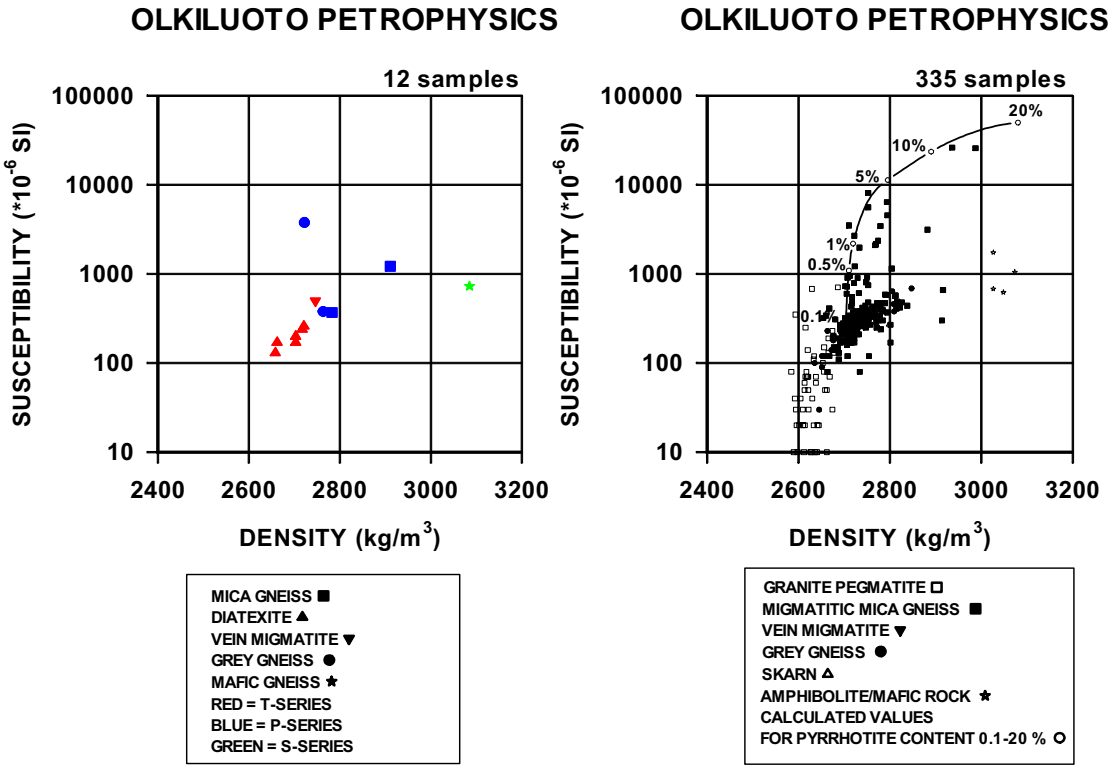

Figure 3-1. *Susceptibility vs. density, a) samples 234 – 245, boreholes OL-KR22 and OL-KR22B, b) data from previously examined deep boreholes OL-KR1 – OL-KR6, minidrill samples and shallow boreholes.*

Since the samples are mainly paramagnetic (susceptibility < $1000 \cdot 10^{-6}$ SI), they usually do not carry significant remanent magnetization. The measured remanence values are typically below 50 mA/m, being below the practical detection limit of the measuring device. However, there are two clearly higher remanence values, 410 and 2080 mA/m, related to previously described ferrimagnetic samples 243 and 234. The determined orientations of the remanent magnetization for these samples are 108.4°/60.3° and 213.2°/55.7° (declination/inclination).

3.2 Electrical properties and porosity

The samples are poor electric conductors with resistivity values ranging from thousands to hundreds of thousands of ohmmeters. There is a reverse correlation between porosity and resistivity as indicated in Fig. 3-2a. T series diatexitic gneiss and veined gneiss samples appear to be most porous, having also the lowest resistivity values. Opaque minerals may also have a slight effect in resistivity, as indicated in Fig. 3-2b, however this relation is not as significant.

a) b)

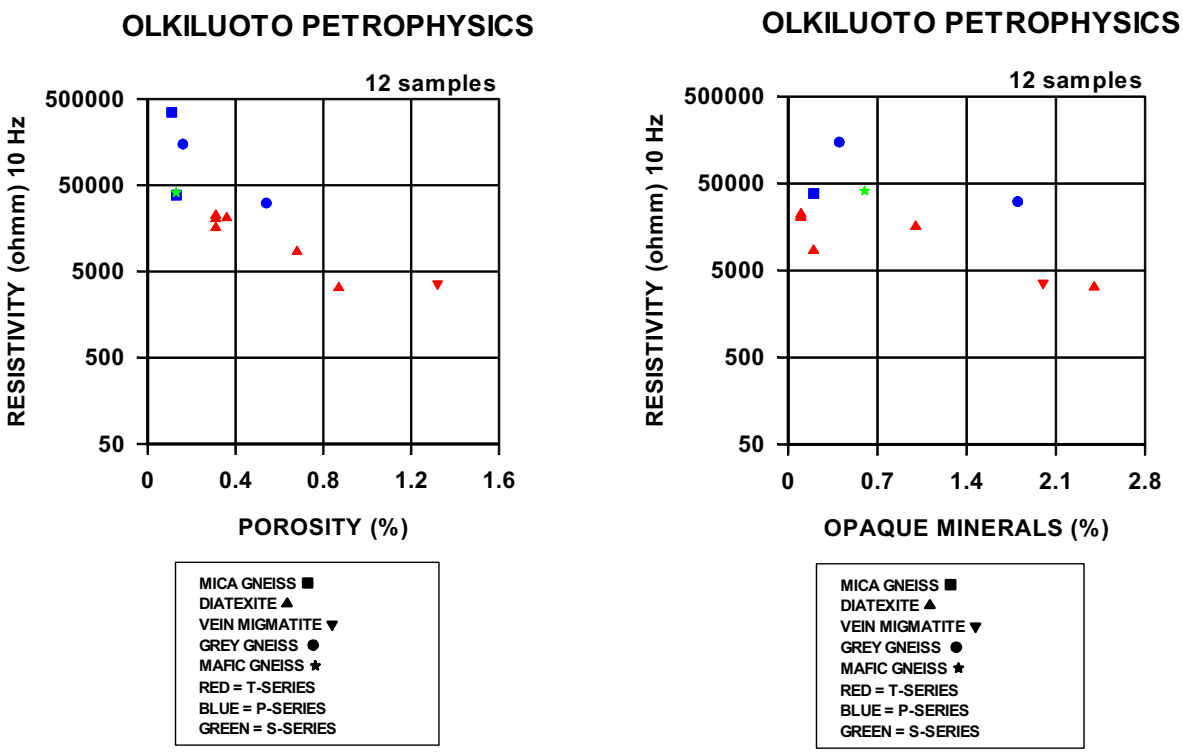

Figure 3-2. *Effect of porosity and content of opaque minerals in electric resistivity, a) porosity vs. resistivity, b) opaque minerals vs. resistivity, OL- KR22 and OL-KR22B.*

3.3 P-wave velocity

P-wave velocity of rocks depends on their porosity and mineral composition. Furthermore, the rocks in Olkiluoto, especially mica gneisses, veined gneisses and diatexitic gneisses are often anisotropic, resulting anisotropy also in P-wave velocity. Typically the highest values are measured along the foliation and the lowest ones perpendicular to it. Measured P-wave velocities are 4830 – 6670 m/s, indicating typically rather unfractured and unaltered crystalline rocks. The porosity vs. P-wave velocity diagram (Fig. 3-3) indicates that velocity is clearly affected by porosity. The highest velocity value is measured from the single S series mafic gneiss (sample 236) and the lowest one from the most porous T series veined gneiss (sample 237). Mica gneisses, diatexitic gneisses and TGG gneisses can not be unambiguously distinguished according to these P-wave velocity data.

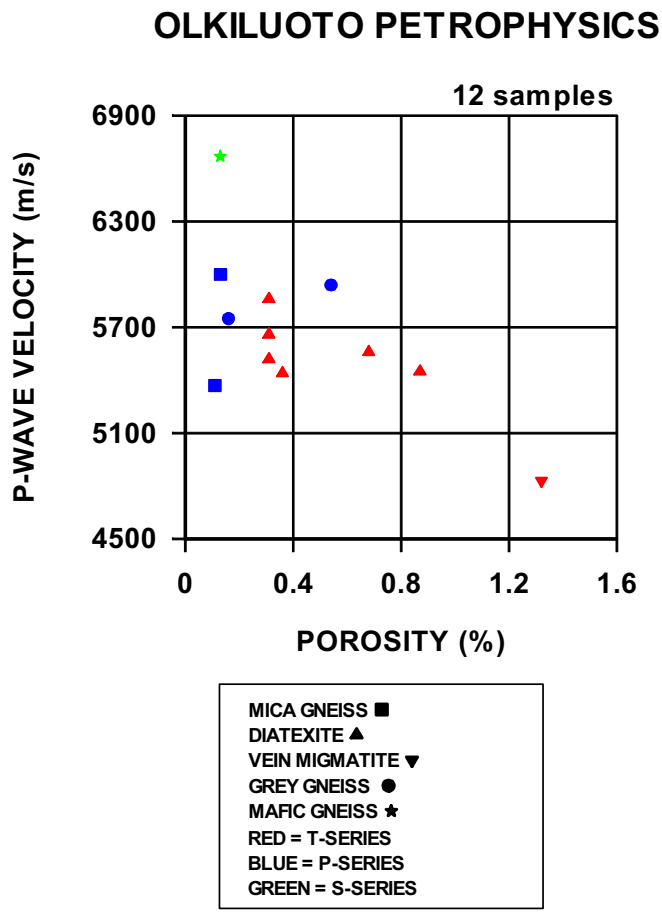

Figure 3-3. *Porosity vs. P-wave velocity, OL-KR22 and OL-KR22B.*

4 FRACTURE MINERALOGY

The account on fracture mineralogy of drill core OL-KR22 aims to following targets:

1. Determinate the position and character of all the open fractures in drill core sample
2. Produce geological classification of the fracture types
3. Make macroscopic identification of fracture filling phases
4. Visually estimate of filling thicknesses of the open fractures
5. Approximation the percentage that the fracture mineral phase coats of the fracture plain area.
6. Characterize the occurrence of cohesive/semi cohesive fracture mineral phases on the fracture plains (cf. chlorite, sericite, graphite, quartz) and the corroded surfaces
7. Make observations of obvious water flow on the fracture plain

Figure 4-1 summarizes the information of the fracture mineralogy, filling characteristics and observations of lithology (logged by A. Kärki), hydrothermal alteration (K. Front and M. Paananen, 2006), zone descriptions (S. Paulamäki et al, 2006) and water conductivity measurements (Pöllänen et al, 2005).

The drill hole OL-KR22 contains 1886 fractures in total, which indicates a relatively dense fracturing; 3.8 fractures/metre. The chief fracture minerals include illite, kaolinite, unspecified clay phases (mainly illite, chlorite, smectite-group), iron sulphides (mainly pyrite, minor pyrrhotite) and calcite. The occurrence of main fracture fillings are given in the Figure 4-1.

In addition to the above mentioned phases, graphite, idiomorphic quartz, sericite, iron-oxides and oxy/hydro-oxides are present in a number of fractures. The fracture plains are occasionally covered by cohesive chlorite, which typically forms the underside for the above-mentioned phases (Fig. 4-1).

Eight zone intersections have been reported from drill core OL-KR22. Most part of those zones are located at drill core length less than 200 metres (Fig. 4-1), which is marked by hydrothermal kaolinite-calcite-sulphide fracture sequences and also contains zone of pervasive illite and kaolinite alteration.

4.1 Fracture fillings at the major pervasive alteration zones

Pervasive illitic alteration forms two zones (see Table 4-2), which range from 10 to 28 m in core length. The pervasively altered zone at length 40 -57 m contains both strong illite and kaolinite alteration. The deeper pervasive illite zone at 385 – 395 m matches with a peak in water conductivity.

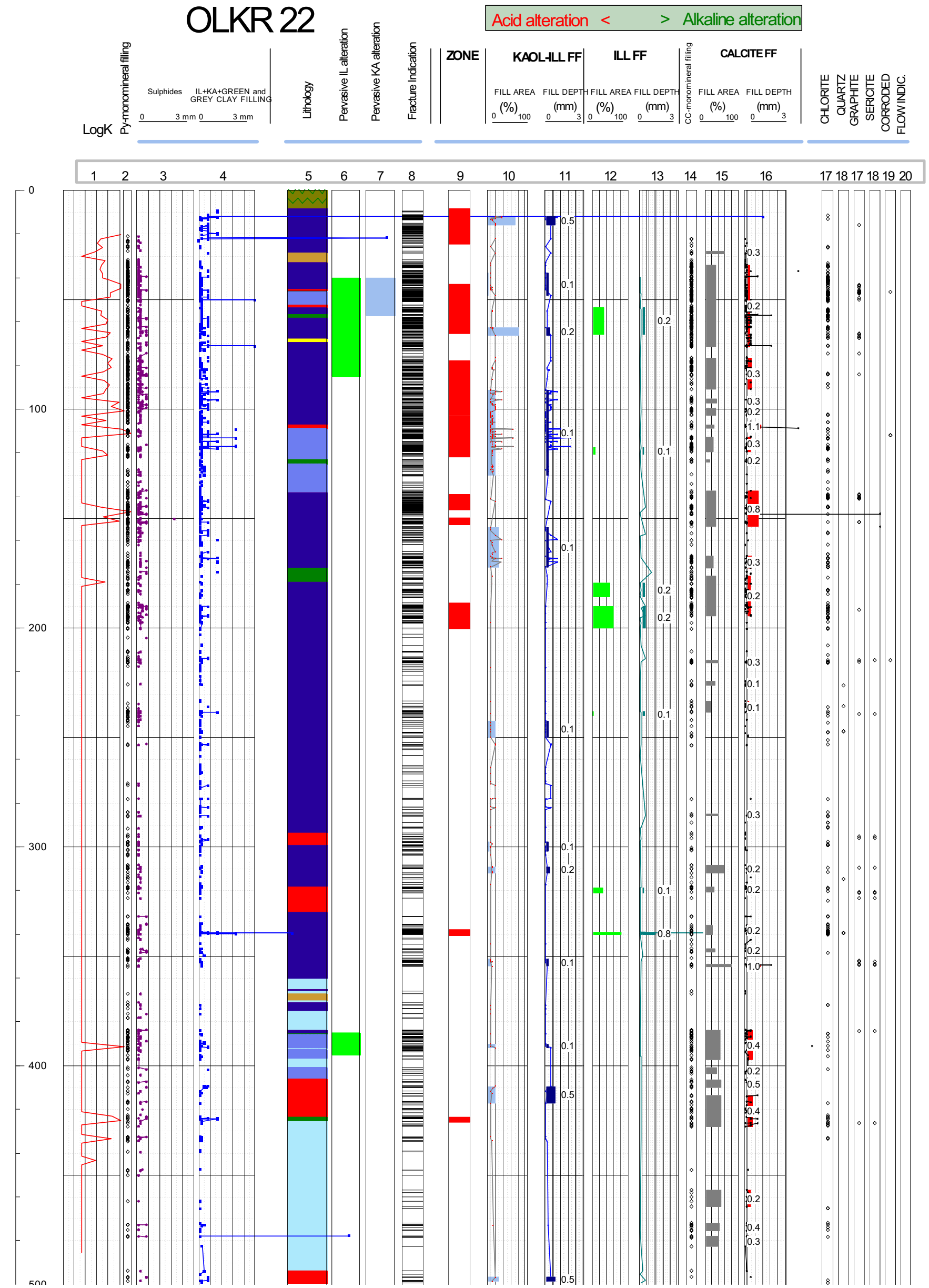
OLKR 22
Acid alteration < > Alkaline alteration
LogK
Py-monomineral filling
Sulphides
IL+KA+GREEN and GREY CLAY FILLING
0 3 mm 0 3 mm
Lithology
Pervasive IL alteration
Pervasive KA alteration
Fracture Indication
ZONE
KAOL-ILL FF
ILL FF
CALCITE FF
FILL AREA (%) FILL DEPTH (mm)
CC-monomineral filling
CHLORITE
QUARTZ
GRAPHITE
SERICITE
CORRODED
FLOW INDIC.
1 2 3 4 5 6 7 8 9 10 11 12 13 14 15 16 17 18 17 18 19 20
0
100
200
300
400
500

Figure 4-1.

Table 4-1. *Explanations of the columns in Fig. 4-1.*

Column No.	Explanation
1	Water conductivity measurement with 2 m packer interval. data from Pöllänen, Pekkanen, Rouhiainen 2005
2	Sulphide as monomineralic fracture filling
3	Sulphide fracture filling (thickness of filling on scale 0 - 3 mm)
4	All clay phases in fracture including hydrothermal and secondary phases (thickness scale 0 - 3 mm)
5	Lithology of drill core, see legend for the lithology on the right. Data logged by A. Kärki.
6	Pervasive illitic alteration of the rock Data from K. Front & M. Paananen 2006.
7	Pervasive kaolinite alteration of rock . Data from K. Front & M. Paananen 2006.
8	Fracture density
9	Deformation zone intersection. Brittle fault zone intersection, brittle joint cluster intersection, semi-brittle fault intersection Data from Paulamäki et al 2006.
10	Percentage[1] of kaolinite illite of the fracture plain area in drill core section (scale: 0 -100 %)
11	Thickness[2] of kaolinite-illite filling in fracture plain area (scale: 0 -3 mm).
12	Percentage[1] of illite of fracture plain in drill core section area (scale: 0 -100 %).
13	Thickness[2] of illite filling on fracture plain area (scale: 0 -3 mm).
14	Occurrence of calcite as monomineralic fracture filling
15	Percentage[1] of calcite of the fracture plain in drill core section area (scale: 0 -100 %).
16	Thickness[2] of calcite on fracture plain in drill core section (scale: 0 -3 mm)
17	occurrence of chlorite in fracture plain
18	occurrence of quartz in fracture plain
21	occurrence of graphite in fracture plain
22	occurrence of sericite in fracture plain
23	occurrence of corrosion on fracture plain
24	Indication of flow marks on fracture plain

The hydrothermal alteration zones have relatively dense fracturing and most of the fractures are chloritic. All these zones contains also the other types of filling phases, mainly sulphides, clay minerals, calcite and graphite, of which particularly the last one is widespread in fractures at length 17 – 43 m, thus it covers the alteration zone only partially.

Table 4-2. *Pervasive illite and kaolinite alteration zones in bore hole OL-KR22.*

Start (m)	End (m)	Core length (m)
Illite alteration		
40	57	17
57	85	28
385	395	10
Kaolinite alteration		
40	57	17

4.2 Fracture fillings outside the pervasively altered zones

At the zones where drill hole cross cuts fracture zones of second-rate hydrothermal activity, the hydrothermal overprint on lithology is typically meagre; only the fractures contain the alteration derivatives. These types of fracture zones are described next within three categories 1) kaolinite-illite fractures 2) illite fractures and 3) calcite fractures.

1. Kaolinite-illitic fracture filling sequences

Fracture sets in which kaolinite ± illite is present as major filling phase. Typically these fractures contain other clay phases, calcite and sulphides in the same assemblages. The clay fillings are thick particularly at the core length 109 – 118 m (Table 4-3), which also is a zone of higher water conductivity. Kaolinite-illite fracture fillings at core length 309 – 311 m and 408 – 416 m are pronounced and they are accompanied by sulphides and calcite.

Table 4-3. *Kaolinite- illite fracture filling zones. Highlighted in grey is the zone in which the water conductivity value is raised.*

Start (m)	End (m)	Average filling thickness (mm)	Core length (m)
12.1	16.0	0.5	3.9
37.8	48.1	0.1	10.3
62.8	66.3	0.2	3.5
91.1	130.2	0.1	39.1
154.2	172.1	0.1	17.9
242.5	250.0	0.1	7.5
297.7	302.0	0.1	4.3
309.1	311.8	0.2	2.7
351.4	354.6	0.1	3.2
390.1	391.8	0.1	1.7
409.4	417.2	0.5	7.8
496.6	498.5	0.5	1.9

2. Illitic fracture filling sequences

The zones in which illite is the predominating filling phase (Table 4-4) are relatively tiny. Distinguished is the illitic cross section 339 – 340 m, which coincides with a water conductivity peak and where the fractures contain sulphides, thick clay fillings, calcite and quartz, the last one as result of silicification.

Table 4-4. *Illite fracture filling zone. Highlighted in grey is the zone in which the water conductivity value is raised.*

Start (m)	End (m)	Average filling thickness (mm)	Core length (m)
53.5	65.8	0.2	12.4
117.6	120.8	0.1	3.3
179.2	185.8	0.2	6.6
190.2	200.1	0.2	9.9
238.3	240.2	0.2	1.9
318.5	321.1	0.1	2.6
339.0	340.1	0.8	1.1

2. Calcitic fracture filling sequences

The calcitic fracture filling sequences are composed of hair dykes or stock works in which the amount of calcite can reach tens of percents of the rock volume. Typically those fracture zones, which have calcite as major phase, are characterized by higher fracture density than in the zones in which the influence of hydrothermal activity is insignificant.

Two main zones of carbonatization occurs; 33.7 – 194 m and 308 – 428 m (Table 4-5). In both these zones calcite occurs in fracture sequences form 1 to 37 meters. The first mentioned carbonatised transverse encloses the kaolinite-illite pervasive and the fracture-related alteration zones

The total core length of the calcite fracture sequences is 180 metres (= 36 % of whole core length). Special attention is subjected to the thick clay filled zones at 107 -108 m, 142 – 151 m, 353 – 354 m, 413 – 427 m, which all contain thick calcite fillings/calcite stockwork and are, excluding the depth 353 - 354 m, linked with water conductivity peaks.

Table 4-5. *Calcite fracture filling zones. Highlighted in grey are the zones which represent advanced carbonatization.*

Start (m)	End (m)	Average filling thickness (mm)	Core length (m)
27.7	28.8	0.3	1.1
34.1	71.6	0.2	37.6
76.4	90.8	0.3	14.4
95.3	97.2	0.3	1.9
99.7	102.9	0.2	3.3
107.3	108.6	1.1	1.4
112.6	119.3	0.3	6.8
122.9	124.0	0.2	1.2
137.2	153.8	0.8	16.6
167.0	172.5	0.3	5.4
176.0	194.5	0.2	18.4
214.7	216.0	0.3	1.3
224.1	226.4	0.1	2.3
233.4	238.5	0.1	5.1
284.8	285.9	0.3	1.1
308.3	311.8	0.2	3.6
318.1	320.6	0.2	2.5
335.8	340.1	0.2	4.3
346.4	348.2	0.2	1.8
353.8	354.8	1.0	1.0
383.6	397.2	0.4	13.6
401.0	403.5	0.2	2.5
406.6	409.9	0.5	3.4
413.5	427.8	0.4	14.3
456.7	464.5	0.2	7.8
472.0	475.5	0.4	3.4
478.0	482.5	0.3	4.5

2. Sulphidised fracture filling sequences

Sulphides are commonly present among the fracture filling assemblages and form also mono mineral fillings all along the drill core sample. It is possible to distinguish a continuous sulphidic zone from core length 34 m to 220 m. In addition there are number of other sulphidic fracture sequences, which have kaolinite-illite and calcite as major phases.

4.3 Iron-oxides and oxy-hydroxides in fracture assemblages

Iron oxides and oxy-hydroxides occur in 21 fractures. They form red-brown coloured fillings at surficial zone, core length 9.53 – 18.95 m. (Table 4-6). Texturally iron-oxide/hydroxide phases are identified as haematite and Fe-hydroxides (goethite, limonite). The oxidized zone contains thick clay filling and a kaolinite- illite alteration zone at core length 11 – 15 m.

Table 4-6. *List of iron oxide and oxy-hydroxide bearing fractures and their hosting lithology in bore hole OLKR22.*

DGN	9.53		DGN	15.32
DGN	9.65		DGN	15.78
DGN	11.29		DGN	15.89
DGN	11.4		DGN	15.98
DGN	11.44		DGN	16.71
DGN	11.54		DGN	16.86
DGN	12.09		DGN	17.02
DGN	12.14		DGN	17.13
DGN	12.18		DGN	17.24
DGN	12.49		DGN	17.36
DGN	12.7		DGN	17.42
DGN	12.76		DGN	17.46
DGN	12.88		DGN	17.53
DGN	12.98		DGN	17.6
DGN	13.08		DGN	17.64
DGN	13.1		DGN	17.84
DGN	13.24		DGN	18.3
DGN	13.38		DGN	18.38
DGN	13.61		DGN	18.53
DGN	14.4		DGN	18.61
DGN	14.47		DGN	18.95
DGN	15.25			

4.4 Relationship between fracture filling data and calvanic connection measurements

Electrical measurement data (Lehtonen 2006) on the galvanic connections concerning the boreholes in Table 4-7. All the groundings from OL-KR22 represent strong (green in Table 4-8) and weak (yellow) galvanic connections. The relationship of fracture fillings/alteration data and results of electric measurements are brought together in Table 4-8.

Table 4-7. *List of the bore holes in which the data of galvanic connections is available.*

OL-KR1
OL-KR2
OL-KR4
OL-KR6 - 8
OL-KR10
OL-KR13 - OL-KR14
OL-KR19
OL-KR22 -25
OL-KR27 – 32

Table 4-8. *Galvanic connections grounded form OL-KR22 (connecting grounding core lengths given in rows) to the bore holes OL-KR4, KR8, KR28 and KR29. The charge potentials are reported (Lehtonen 2006) to fall into category strong (highligted in green and "weak" (highlighted in yellow).*

KR22	KR4	KR8	KR28	KR29	Fracture filling in KR22
150	80				Bulky calcite, sulphides, water conductivity peak
190	116				Fracture illite, calcite, graphite, sulphides
310	314				tiny zone of fracture kaolinite, calcite, sulphides, graphite
450	368				-
440	383				-
185-200			179		Zone of fracture illite, calcite, sulphides and graphite, water conductivity peak within the zone
265-285			245		-
310			368		Tiny zone of fracture kaolinite, calcite, sulphides, graphite
445			442		-
310				130	Tiny zone of fracture kaolinite, calcite, sulphides, graphite
310				213	See above
310-				335	See above
75		80			Pervasive illite alteration, calcite, sulphides, water conductivity peak
75-(160)		162			Pervasive illite alteration, calcite, sulphides, water conductivity peak within the zone
152		0			bulky calcite, sulphides, water conductivity peak

5 SUMMARY

The boreholes OL-KR22 and –KR22B start in the central part of the Olkiluoto study area from the wide migmatite unit dominated by diatexitic gneisses. The drill holes intersect down to the drilling length of 360 m a rather monotonous diatexitic gneisses which are intruded by a couple of wide pegmatitic dykes and have several homogeneous mica gneiss and mafic gneiss interbeds. Below those, down to the drilling length of 422 m a fluctuating section of veined gneisses with narrow mica gneiss interbeds is located. The lowermost part of the core sample is composed of rather homogeneous mica gneisses with various migmatite subsections.

Whole rock chemical composition is analysed in detail from12 samples. Seven of those are migmatites of the T series, four are gneisses and migmatites of the P series and one is mafic, S-type gneiss. The T type diatexitic gneiss and veined gneiss samples give an extensive overview of the whole series. SiO_2 concentration varies from 58% analysed from a biotite rich veined gneiss to ca. 73% analysed from a leucocratic diatexitic gneiss. The silicity controls directly the other major element concentrations as typical for the T series. One mafic gneiss sample is a member of the S-series and the most mafic variant analysed from this category. It contains only 43% SiO_2 and ca. 10% CaO but, in other respects, it is typical mafic gneiss of the S series. The P series is represented by TGG gneiss, diatexitic gneiss and mica gneiss samples. Content of phosphorus exceeds 0.4%, given as P_2O_5, in every of those. The content of aluminium is constantly ca. 17% despite of the change in silicity or migmatite structure but the other major element concentrations show a clear decreasing trend which is directly controlled by the increase in silicity. Migmatites are not numerous in the P series but their major element concentrations fall systematically to the same numbers which are typical for the P-type gneisses. The P-type TGG gneiss sample contains less than 60% SiO_2 and thus it belongs to the subgroup of less silicic variants of the series. P_2O_5 concentration is ca.0.45% and CaO concentration exceeds 3% which are typical numbers for these gneisses. The mica gneiss samples studied in detail represent both extremities in this subsequence of the P series. SiO_2 concentration of the former is ca. 50% and of the latter ca. 60. P_2O_5 concentration decreases from 1.4% to 0.7% and CaO from 5% close to 4% as silicity increases and also the other major element concentrations are strictly in anticipated numbers.

The additional XRF major element analyses were made from samples that were taken by 5 m average interval from this core. The aim of these analyses was to clarify the distribution and proportions if individual rock series. The chemical border between T and P series is set at the 0.2% content of P_2O_5. The border between the members of the T and S series is set at the 2% content of CaO. According to this test the members of the P and T series are located at all depths in the drill hole. The members of the T series seem to compose 70%, the members of the P series 20% and the members of the S series the remaining 10% of the bedrock volume intersected by the drill hole OL-KR22. However, the 5 m sample interval has proved to be too coarse in determination of borders between primary sections of original rock layers or sequences of individual rock series.

The diatexitic T-type gneisses belong to the more acidic half of the series as SiO_2 varies between 63 and 73% and the content of quartz between 27% and 43%, content of plagioclase between 11% and 27% and K-feldspar between 11 and 25%. The proportion of biotite or total number of biotite and chlorite, if the latter is present, varies between 10 and 25%. Cordierite has been present in the every sample but now it is pinitic for the most part, and sillimanite belongs to the assemblage as a minor component. The diatexitic gneisses are rather coarse-grained and poorly foliated. Features of rough metamorphic banding can be imagined but the dark bands are more or less irregular, 2 – 4 mm wide zones into which the mafic minerals are concentrated. The veined gneiss of the T series is less silicic than any of the diatexites and SiO_2 content of 59% is rather low number among the whole T series, too. The gneiss is evidently darker and contains ca. 40% biotite. Quartz content is 22%, plagioclase 12% and K-feldspar 10%. The10% content of pinite and small amount of sillimanite are also typical. The sample is relatively coarse-grained and metamorphic banding in the paleosome of the rock is well developed. Dark bands are wavy and border the leucocratic parts or veins.

The mafic S-type gneiss is composed near to completely of hornblende the proportion of which is 82%. Biotite content is 10% and chlorite 5%. In addition, the sample contains only a trace amount of plagioclase and apatite. The mafic gneiss is medium-grained with average diameter of amphibole grains close to 2 mm. The amphibole grains are roundish and the texture resembles granoblastic texture of felsic, medium-grained gneisses.

The P-type diatexitic gneiss belongs to an infrequent subgroup of migmatites. The gneiss includes 64% SiO_2 and is the most silicic variety in its category. Quartz content of 36%, plagioclase of 11%, K-feldspar of 19% and biotite of 5% are not anomalous numbers for the P-type migmatites but high content of muscovite (8%) is not typical. This diatexite is medium-grained, granoblastic and not evidently foliated. Mafic minerals are concentrated into material which borders 5 – 10 mm wide, roundish quartz-feldspar aggregates making the whole structure similar to certain porphyry-like rocks. The Mica gneisses of the P series represent both extremes in the sequence as the other includes SiO_2 only 50.5% and the other 60.5%. Quartz contents are 26% and 30%, plagioclase contents 27% and 36%, and biotite contents 36% and 28% in the less silicic and more silicic sample, respectively. Rather high content of apatite is typical likewise the total lack of K-feldspar. The mica gneisses are fine-grained and poorly foliated. Features of a weak metamorphic banding can be imagined. The P-type TGG gneiss includes 59% SiO_2 and thus it belongs to the less silicic type in the sequence. Quartz content of 14% is typical value for this kind of rocks. Low contents of plagioclase and both K-feldspar and biotite will be explained by high contents of chlorite and saussurite. A couple percent of apatite and sphene belong to these rocks. The gneiss is granoblastic and medium-grained. Quartz-feldspar aggregates with diameters varying from 5 to 10 mm are typical elements for that. These aggregates or patches are surrounded by a more mafic “groundmass” which contains the most part of micas but the foliation of this mica bearing material is poorly developed.

Petrophysical properties were measured from 12 samples. Their measured density values range between 2658 and 3085 kg/m^3. The highest value is measured from the

sample 236, which is mafic gneiss. From the rock types, diatexite samples appear to be lighter than the other samples.

Most of the samples are paramagnetic or weakly ferrimagnetic with susceptibility values ranging from $130 \cdot 10^{-6}$ SI to $3780 \cdot 10^{-6}$ SI. Most of the samples measured correspond rather well with the paramagnetic gneiss population of the older data. There are two slightly ferrimagnetic samples, (one P type TGG gneiss and one P-type mica gneiss), indicating small amounts of ferrimagnetic minerals. The measured remanence values are typically below 50 mA/m, being below the practical detection limit of the measuring device. However, there are two clearly higher remanence values, 410 and 2080 mA/m, related to previously described ferrimagnetic samples.

The samples are poor electric conductors with resistivity values ranging from thousands to hundreds of thousands of ohmmeters. There is a reverse correlation between porosity and resistivity. T-type diatexite and veined gneiss samples appear to be most porous, having also the lowest resistivity values. Opaque minerals may also have a slight effect in resistivity, however this relation is not as significant.

Measured P-wave velocities are 4830 – 6670 m/s, indicating typically rather unfractured and unaltered crystalline rocks. The porosity vs. P-wave velocity diagram indicates that velocity is clearly affected by porosity. The highest velocity value is measured from a single S-type mafic gneiss and the lowest one from the most porous veined gneiss of the T series. Mica gneisses, diatexites and TGG gneisses can not be unambiguously distinguished according to the P-wave velocity data.

The drill hole OL-KR22 has relatively dense fracturing; 3.8 fractures/metre. Pervasive illitization concerns 11 % of the total core length and 36 % of the bore hole length has calcite as major constituent in fracture fillings. The chief fracture minerals include illite, kaolinite, unspecified clay phases, iron sulphides and calcite. Sulphides occur in fracture plains all along the drill core, but at the core length interval 34 – 220 m its occurrence is more intense. Graphite occurs abundantly in a sequence at the core length 20 - 50 m, and sporadically all along the drill core. Idiomorphic quartz and sericite are present in a number of fractures. Iron-oxides and oxy/hydro-oxides are met in few fractures at core length 9.53 – 18.95 m. The fracture plains are occasionally covered by cohesive chlorite, which typically forms the underside for the other filling phases.

The frequency of fracturing is clearly higher at the first 200 meters of the core length. This depth interval contains zone intersections, pervasive illite and kaolinite alteration zones and abundant calcite.

At the upper 200 m of the core length the water conductivity peaks join with the hydrothermal zones and at this interval the calcitic fracture filling sequences are indicators for the increased water conductivity. Especially the thick clay filled zones at 107 -108 m, 142 – 151 m, 353 – 354 m, 413 – 427 m contain thick calcite fillings/calcite stockworks.

REFERENCES

Front, K. & Paananen, M. 2006. Hydrothermal alteration at Olkiluoto: mapping of drill core samples. Working Report 2006-59. Posiva Oy, Olkiluoto.

Gehör, S., Kärki, A., Määttä, T., Suoperä, S. & Taikina-aho, O., 1996. Eurajoen Olkiluodon kairausnäytteiden petrologia ja matalan lämpötilan rakomineraalit. Työraportti PATU-96-42. Posiva Oy, Helsinki.

Korsman, K., Koistinen, T., Kohonen, J., Wennerström, M, Ekdahl, E., Honkamo, M, Idman H. & Pekkala, Y. (editors) 1997. Suomen kallioperäkartta -Berggrundskarta över Finland -Bedrock map of Finland 1: 1 000 000. Geologian tutkimuskeskus, Espoo, Finland.

Kärki, A. & Paulamäki, S. 2006. Petrology of Olkiluoto. Posiva 2006-2. Posiva Oy, Olkiluoto, 77 p.

Lehtonen, T. 2006. Visualization and Interpretation of the Year 2004 Mise-a-la-Masse Survey Data at Olkiluoto Site. Working Report 2006-08. Posiva Oy, Olkiluoto.

Mattila, J. 2006. A System of Nomenclature for Rocks in Olkiluoto. Working report 2006-32. Posiva Oy, Olkiluoto. 16 p.

Niinimäki, R. 2002. Core drilling of deep borehole OL-KR22 at Olkiluoto in Eurajoki 2002. Working Report 2002-59. Posiva Oy, Olkiluoto. 199 p.

Paulamäki, S., Paananen, M., Gehör, S., Kärki, A., Front, K., Aaltonen, I., Ahokas, T., Kemppainen, K., Mattila, J. & Wikström, L. 2006. Geological model of the Olkiluoto site, version 0. Working Report 2006-37. Posiva Oy, Olkiluoto.

Pöllänen, J., Pekkanen, J., Rouhiainen, P. 2005. Difference flow and electric conductivity measurements at the Olkiluoto site in Eurajoki, boreholes KR19 – KR28, KR19B, KR20B, KR22B, KR23B, KR27B and KR28B. Working report 2005-52. Posiva Oy, Olkiluoto.

Suominen, V. 1991. The chronostratigraphy of southwestern Finland with special reference to Postjotnian and Subjotnian diabases. Geological Survey of Finland Bulletin 356, 100 p.

Suominen, V., Fagerström, P. & Torssonen, M. 1997. Pre-Quaternary rocks of the Rauma map-sheet area (in Finnish with an English summary). Geological Survey of Finland, Geological Map of Finland 1:100 000, Explanation to the maps of Pre-Quaternary rocks, Sheet 1132, 54 p.

Veräjämäki, A. 1998. Pre-Quaternary rocks of the Kokemäki map-sheet area (in Finnish with an English summary). Geological Survey of Finland, Geological Map of Finland 1:100 000, Explanation to the maps of Pre-Quaternary rocks, Sheet 1134, 51 p.

APPENDICES

Appendix 1.

File KR22_APP1 in the disk enclosed. The Appendix contains the results of whole rock chemical analyses.

Appendix 2.

File KR22_APP2 in the disk enclosed. The Appendix contains the results of whole rock XRF analyses.

Appendix 3.

File KR22_APP3 in the disk enclosed. The Appendix contains the results of modal mineral composition analyses.

Appendix 4. Petrophysical parameters, drill core OL-KR22.

								RESISTIVITY VALUES (Ωm)			IP-ESTIMATES		
HOLE	**SAMPLE**	**FROM**	**TO**	**D(kg/m^3)**	**K(μSI)**	**J(mA/m)**	**P-wave (m/s)**	**R0.1[Ωm]**	**R10 [Ωm]**	**R500[Ωm]**	**PL (%)**	**PT (%)**	**Pe(%)**
KR22	OL.234	69.07	69.16	2911	1220	410	5370	resistivities > 334864					0.11
KR22	OL.235	93.25	93.36	2658	130	50	5450	3620	3240	2920	10	19	0.87
KR22	OL.236	124.37	124.46	3085	730	30	6670	46100	41100	27600	11	40	0.13
KR22	OL.237	127.85	127.95	2746	500	100	4830	3840	3590	3170	7	17	1.32
KR22	OL.238	202.59	202.69	2703	170	30	5520	17900	16100	14700	10	18	0.31
KR22	OL.239	227.85	*	2721	260	10	5660	21600	20500	17600	5	19	0.31
KR22	OL.240	288.10	288.19	2717	240	30	5440	22000	21000	18300	5	17	0.36
KR22	OL.241	343.03	343.10	2703	200	30	5860	23900	22400	19200	6	20	0.31
KR22	OL.242	369.86	369.94	2783	370	20	6000	41300	38400	30300	7	27	0.13
KR22	OL.243	433.07	433.17	2722	3780	2080	5940	35800	31100	24200	13	32	0.54
KR22	OL.244	477.90	477.96	2662	170	10	5560	8410	8520	7400	0	12	0.68
KR22B	OL.245	31.16	31.26	2763	380	20	5750	resistivities > 138884					0.16

D = density
K = magnetic susceptibility
J = remanent magnetization
P-wave = velocity of seismic P-wave
R0.1 = electric resistivity, 0.1 Hz frequency
R10 = electric resistivity, 10 Hz frequency
R500 = electric resistivity, 500 Hz frequency
PL = IP effect = 100*(R0.1-R10)/R0.1
PT = IP effect = 100*(R0.1-R500)/R0.1
Pe = effective porosity

* The depth value was not readable from the sample